https://doi.org/10.5194/hess-2023-292
Preprint. Discussion started: 5 January 2024

Hydrology and Earth System Sciences
Discussions

Improving the internal hydrological consistency of a process-based solute-transport model by simultaneous calibration of streamflow and stream concentrations

Jordy Salmon-Monviola[1], Ophélie Fovet[1], Markus Hrachowitz[2]

[1] UMR SAS, INRAE, Institut Agro, Rennes, France

[2] Department of Water Management, Faculty of Civil Engineering and Geosciences, Delft University of Technology, Stevinweg 1, 2628CN Delft, Netherlands

Correspondence to: J. Salmon-Monviola (jordy.salmon-monviola@inrae.fr)

Abstract. Improving the consistency of hydrological models, i.e. their ability to reproduce observed system dynamics, is required to increase their predictive power. As the use of streamflow data for calibration is necessary but not sufficient to constrain model and warrant model consistency, other strategies must be considered, in particular the use of additional data sources. The aim of this study is to test whether simultaneous calibration of dissolved organic carbon (DOC) and nitrate (NO_3^-) concentrations along with streamflow improves the hydrological consistency of a parsimonious solute-transport model. A multi-objective and multi-variable approach was used to evaluate the model in an intensive agricultural headwater catchment. Our results showed that using daily stream concentrations of DOC and NO_3^- together with streamflow data during calibration did not improve the model's ability to accurately predict streamflow for calibration or evaluation periods. However, the internal consistency of the model was improved for the simulation of low flows, groundwater storage and upstream soil storage, but not for the simulation of riparian soil storage. Parameter uncertainty decreased when the model was calibrated using solute concentrations, except for parameters related to fast and slow reservoir flow. This study shows the added value of using multiple data sources in addition to streamflow data for calibration, in particular DOC and NO_3^- concentrations, to constrain hydrological models for a better representation of internal hydrological states and flow. With the increasing availability of solute data from catchment monitoring, this approach provides an objective way to improve the internal consistency of hydrological models that can be used with confidence in scenario evaluation.

Keywords: Hydrological models, Equifinality, Consistency, Multi-objective calibration, Stream DOC and nitrate concentrations, parsimony.

https://doi.org/10.5194/hess-2023-292
Preprint. Discussion started: 5 January 2024

Hydrology and Earth System Sciences
Discussions

1. Introduction

Hydrological models are important tools for short-term forecasting of river flows and long-term predictions for strategic water management planning, as well as for improving understanding of hydrological processes and the complex interactions of water storage and release processes at the catchment scale (Minville et al., 2014; Lan et al., 2020; Bouaziz et al., 2021). In the wide spectrum of modelling, which ranges from simple to complex (Gharari et al., 2014; Hrachowitz and Clark, 2017; Adeyeri et al., 2020), conceptual models, in which only the dominant processes are represented and/or several processes may be lumped into a single expression (Pettersson et al., 2001), are widely used to simulate hydrological dynamics of catchments. Conceptualising the system as a set of storage components connected by fluxes representing the perceived dominant processes of a catchment provides a certain degree of flexibility. The ability to customize these models to the environmental conditions in a given catchment can ensure an appropriate level of complexity to reproduce response patterns of hydrology and water quality (Hrachowitz et al., 2016). Major advantages of conceptual models include their relatively low data and computational requirements, which makes them suitable for studies at different scales or for catchments about which little information is available (Gharari et al., 2014; Huang and Bardossy, 2020). However, ad hoc implementation of conceptual models frequently lacks a plausible theoretical basis and thus a meaningful connection of model structure and parameters to observable quantities when representing integrated system processes (Clark et al., 2016). As such, the ability of models, including conceptual ones, to reproduce a system's dynamics is also undermined not only by random uncertainties in the data, but also by epistemic or ontological uncertainties and thus by limited knowledge of the physical processes that underlie the system's response (Beven and Westerberg, 2011; Gupta et al., 2012; Beven, 2013). These uncertainties and the few observations in a continuous spatial domain make such models ill-posed inverse problems (Pettersson et al., 2001; Beven, 2006; Hrachowitz et al., 2014). In hydrology, frequently referred to as equifinality (Beven, 1993), these insufficient model constraints thus result in many, equally good alternative model solutions. Hydrological models with many parameters thus tend to adapt to errors and to compensate for inadequate representation of processes through the model parameters (Wang et al., 2012). For example, well-predicted river discharge is often associated with poorly predicted evaporation fluxes, because evaporation compensates for errors and closes the hydrological balance (Minville et al., 2014). Thus, deceptively high calibration accuracy may reflect mathematical fitting of an often overparameterized model, which may generate undesirable internal dynamics that decrease accuracy in independent evaluation periods (Hrachowitz et al., 2014; Fovet et al., 2015a). Robust model calibration and evaluation procedures are thus needed to address issues of parameter identifiability (Beven, 2006; Guillaume et al., 2019) and transferability (Hartmann and Bárdossy, 2005; Minville et al., 2014; Kreye et al., 2019), and to avoid models that act as "mathematical marionettes" dancing to match the calibration data (Kirchner, 2006) but often fail to reproduce internal system dynamics.

Recently, a trend toward more comprehensive assessment of the structural adequacy of models has emerged during the calibration process (Yen et al., 2014; Rakovec et al., 2016), with the overall goal of improving the representation of multiple hydrological processes in a model (Clark et al., 2011; Gupta et al., 2012; Euser et al., 2015). The rationale behind this goals is the need to obtain the "right answers for the right reasons" (Blöschl, 2001; Kirchner, 2006), which goes beyond simply comparing model predictions to observed streamflow or associated signature measurements (Euser et al., 2013; Fovet et al., 2015a; Rakovec et al., 2016). Indeed, reflecting the results of many studies, Rakovec et al. (2016) showed that streamflow data are necessary but not sufficient to warrant constraining model components by dividing incoming rainfall among storage, evaporation and drainage (Bouaziz et al., 2021). Thus, multiple strategies have been developed to improve the physical realism of conceptual models

https://doi.org/10.5194/hess-2023-292
Preprint. Discussion started: 5 January 2024

(i.e. model *consistency*) (Efstratiadis and Koutsoyiannis, 2010), including using additional data that represent internal hydrological states and fluxes other than streamflow when estimating parameters. Treating the system more holistically (i.e., forcing models to simulate multiple response variables adequately) has considerable potential to improve model accuracy (Hrachowitz et al., 2014). The value of such multi-variable and/or multi-objective strategies has been demonstrated using groundwater levels (Freer et al., 2004; Molenat et al., 2005; Giustolisi and Simeone, 2006; Fenicia et al., 2008), near-surface soil moisture (Brocca et al., 2010; Sutanudjaja et al., 2014; Rajib et al., 2016; Kunnath-Poovakka et al., 2016; López López et al., 2017), saturated contributing areas (Franks et al., 1998; Güntner et al., 1999; Blazkova et al., 2002), snow cover (Gao et al., 2017; Bennett et al., 2019; Riboust et al., 2019), evaporation (Bouaziz et al., 2018; Demirel et al., 2018; Hulsman et al., 2020), streamflow at subcatchment outlets (Moussa et al., 2007), satellite-based total water storage anomalies (Werth and Güntner, 2010; Yassin et al., 2017) and tracer data (Birkel et al., 2011; Capell et al., 2012; Birkel et al., 2015; Kuppel et al., 2018a; Piovano et al., 2019; Stadnyk and Holmes, 2023). Alternately, one may seek to extract more information from available data, for example by developing signatures that represent different aspects of the data (Euser et al., 2013; Gharari et al., 2014; Fenicia et al., 2018).

Simultaneously calibrating hydrological models with streamflow and tracer or other solute concentrations in the stream may decrease their uncertainty and increase their physical plausibility because of the need to reproduce both hydrological and biogeochemical dynamics (Pettersson et al., 2001; Woodward et al., 2013a; Fovet et al., 2015b; Birkel et al., 2017; Strohmenger et al., 2021; Pesántez et al., 2023). The value of this strategy has been demonstrated, for example using concentrations of chloride (Hrachowitz et al., 2013) or nitrate (NO_3^-) and sulphate (Pettersson et al., 2001; Hartmann et al., 2013). This potential is particularly important when the spatial distribution of solutes differs significantly from that of the dynamics of stream concentrations (Woodward et al., 2013a; Shafii et al., 2019), as often observed for dissolved organic carbon (DOC) and NO_3^- (Taylor and Townsend, 2010; Strohmenger et al., 2021). Indeed, previous studies have shown that seasonal variations in DOC and NO_3^- are closely related to fluctuations in the groundwater level in groundwater-fed catchments (Aubert et al., 2013; Birkel et al., 2014; Humbert et al., 2015; Tunaley et al., 2016; Abbott et al., 2018; Birkel et al., 2020; Strohmenger et al., 2020). In contrast, short-term variations in DOC and NO_3^- have been related to the activation of subsurface and surface flow pathways during storm events and the subsequent hydrological connection of DOC-rich and NO_3^--poor riparian soils to the stream, particularly for near-surface soil layers (Dick et al., 2015; Strohmenger et al., 2021).

The objective of this study was thus to test the hypotheses that, by including daily in-stream DOC and NO_3^- concentrations simultaneously in a parsimonious conceptual model in a multi-objective and multi-variable calibration and evaluation strategy, we could increase the model's (1) ability to predict streamflow for calibration or evaluation periods, (2) internal consistency, and (3) reduce the uncertainty in hydrological parameters.

2. Materials and Methods

2.1. Study site

The Kervidy-Naizin catchment is located in western France (48° 0’ N, 2° 5’ W) (Fig. 1) and forms part of the AgrHyS Critical Zone Observatory (Fovet et al., 2018). It is a 4.82 km² headwater catchment of the 12 km² Naizin catchment (Fig. 1), which is drained by a second-Strahler-order intermittent stream that frequently dries up from July to October and has a mean specific runoff (± standard deviation) of 296 ± 150 mm yr^{-1}.

The climate is temperate oceanic, with a mean annual temperature of 11.2 ± 0.6°C and mean annual rainfall of 810 ± 180 mm. The topography is relatively flat, with few slopes reaching a gradient of 5%, and an elevation range of 98-140 m above sea level. The soil is a silty loam 0.5-1.5 m deep, with well-drained Cambisols in the upslope zone and poorly drained Epistagnic Haplic Luvisols and Albeluvisols in the downslope riparian zone (FAO classification (WRB, 2006)). The bedrock consists of a variety of Brioverian schists of low permeability and lies below a fissured and fractured weathered layer of variable thickness 1-30 m deep (Molenat et al., 2005). A shallow, perennial groundwater body develops in the soil and weathered bedrock. Near the river (hereafter, “riparian zone”), the groundwater level fluctuates within 1 m of the surface, while upslope it always remains deeper than 4 m, with an increased seasonal fluctuation that can descend to 6 m in depth (Molenat et al., 2005).

The land use of Kervidy-Naizin consists mainly of agriculture with intensive mixed crop-livestock farming, with maize (36% of the area), cereals (32%) and grasslands (13%), and a high density of livestock (i.e. dairy cattle, pigs and poultry) of 5 livestock units ha^{-1} (Viaud et al., 2018; Casal et al., 2018, 2019). From 2002–2015, mean N inputs on the catchment equalled 257 kg ha^{-1} yr^{-1}, coming from slurry and manure fertilization (69%), inorganic fertilization (21%, mainly ammonium nitrate), cattle excretion in pastures (5%) and nitrogen (N) fixation (5%) (Casal et al., 2019). Kervidy-Naizin is representative of intensive agricultural areas that have an excess of reactive N due to the application of livestock waste and inorganic fertilisers in excess of crop requirements. In this landscape, most DOC and NO_3^- accumulate in riparian-zone soils and groundwater, respectively (Aubert et al., 2013; Strohmenger et al., 2020); thus, biogeochemical and hydrological dynamics and processes in this headwater catchment can be analysed in the context of unlimited DOC and N supply. At the global scale, Kervidy-Naizin is also representative of headwater catchments underlain by bedrock in temperate climates.

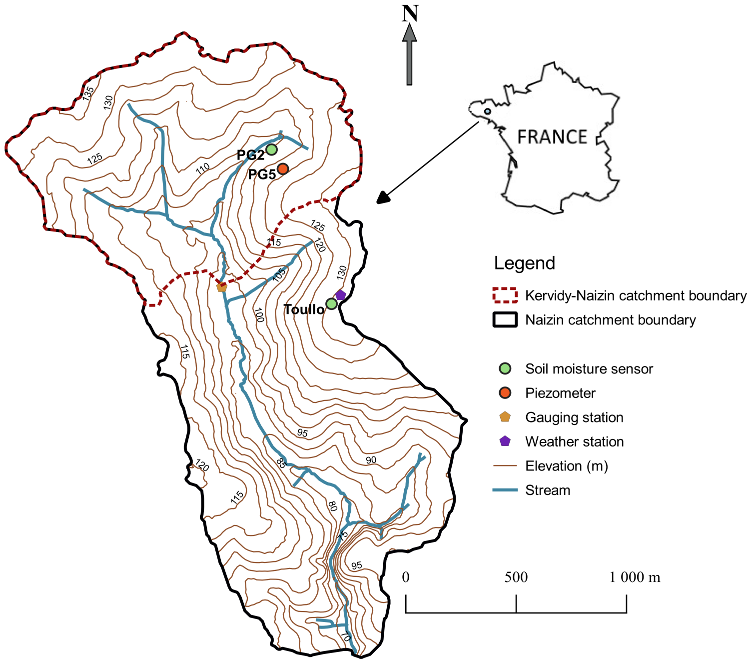

Figure 1. Map of the Kervidy-Naizin catchment (4.82 km^2, western France)

2.2. Data monitoring

We used daily aggregated meteorological and streamflow measurements collected from 2002-2017. The weather station at Kervidy (Cimel Enerco 516i), located ca. 1 km from the outlet of the catchment (Fig. 1), records hourly rainfall, air and soil temperatures, air humidity, global radiation, wind direction and wind speed, which allowed for calculation of potential evapotranspiration using the Penman equation (Penman, 1956). Stream level was recorded every minute at the outlet using a float-operated shaft-encoder level sensor and a data logger (Thalimedes OTT) and then converted to streamflow using a rating curve (Carluer, 1998).

Stream water was manually sampled daily at ca. 17:00 at the outlet station. These instantaneous grab samples were immediately filtered (pore size: 0.22 µm) on site and stored in the dark at 4°C in propylene bottles. Analyses were performed within a maximum of two weeks. NO_3^- concentrations were measured by ionic chromatography (DIONEX DX 100, (ISO, 1995), precision: ±2.5%). DOC was estimated as total dissolved carbon (C) minus dissolved inorganic C, both measured using a C analyser (Shimadzu TOC 5050A, precision: ±5%).

Shallow-groundwater data were collected by a piezometer at mid-slope point (PG5, Fig. 1). The groundwater level at PG5, which has been measured every 15 min (Orpheus OTT) since 2000 using pressure probes, was used because its variations are representative of mean variations in the shallow groundwater in the Kervidy-Naizin. The volumetric soil water content was measured in upland and riparian zones of the catchment using TDR probes. In the upland zone (Toullo station, Fig.1), it was measured at three depths (i.e. 5, 20 and 50 cm), with three replicates per depth, at 30 min intervals from 1 Jan 2016 to 1 Jan 2019; these data were first averaged by depth and then aggregated into daily values. Although the Toullo station lies outside the Kervidy-Naizin catchment, it represents the catchment's soil moisture conditions in the upland zone. In the riparian zone (point PG2, Fig. 1), the volumetric soil water content was measured at a depth of 5 cm, with three replicates, at 30 min intervals from 3 Dec 2013 to 1 Jan 2017; these data were also averaged and then aggregated into daily values.

2.3. Rationale for the solute-transport model

We used a parsimonious semi-distributed solute-transport model, implemented in Python, that was iteratively customized and tested within the DYNAMITE modular modelling framework (Hrachowitz et al., 2014, 2021; Fovet et al., 2015a). The processes are represented by linear or non-linear equations that connect the fluxes to model reservoirs (Beven, 2012). This representation of storage-discharge relationships directly connects water fluxes to biogeochemical processes, which facilitates simultaneous simulation of both water and solute fluxes (Birkel et al., 2017).

2.3.1. Hydrology

The model spatially distinguishes two functionally distinct response units: hillslope and riparian zones. It represents them as two parallel suites of reservoirs connected by a common groundwater reservoir (Fig. 2). The hillslopes are represented as two reservoirs: the rooting-zone reservoir (S_U) [L] and a fast-responding reservoir (S_F) [L] (e.g. preferential flow structures). As riparian zones often have a distinct hydrological function (Seibert et al., 2003; Molenat et al., 2005; Seibert et al., 2009), the model also represents them as two reservoirs: an unsaturated-zone reservoir (S_{UR}) [L] and a fast-responding reservoir (S_R) [L]. The two parallel suites are connected by a slow groundwater reservoir (S_S) [L], characterized by a threshold from which the groundwater feeds the S_{UR} reservoir that represents a groundwater mixing volume (S_{S_mix}) [L]. See Table 1 for the relevant model equations. More detailed model description and justifications for the processes modelled can be found in previous studies (Hrachowitz et al., 2013, 2014, 2015).

The rainfall-runoff model uses daily precipitation (P) [L T^{-1}] and potential evapotranspiration (E_P) [L T^{-1}] to simulate daily specific discharge at the outlet (Q_T) [L T^{-1}]. Upon reaching the soil, P is divided into water that infiltrates into S_U (R_U, Table 1) and excess water by a hillslope runoff-generation coefficient ($C_{H,R}$) routed to S_F (R_F) and S_S (R_P). $C_{H,R}$ is estimated by a logistic function representing the catchment-wide soil water holding capacity in the rooting zone (S_{U_max}), which roughly reflects soil water content at field capacity, and a shape factor (β_H). Percolation of water from S_U to S_S (R_{SS}) is estimated by a linear function of the water storage in S_U and a maximum percolation capacity (P_{max}). Evapotranspiration from S_U (E_U) is estimated by a linear function of the relative soil moisture and a transpiration threshold (L_P), which is the fraction of S_{U_max} below which potential evapotranspiration (E_P) is constrained by the water available in S_U.

Fast reservoir S_F receives water (R_F) from S_U (Table 1, Eq. (8)) and drains into reservoir S_{UR} according to a linear storage-discharge relationship that is controlled by parameter k_F. Slow reservoir S_S is recharged by R_{SS} and R_P from S_U and slowly drains according to a linear storage-discharge relationship that is controlled by parameter k_S. The water drained from S_S is redistributed between S_{UR} and the stream according to parameter f_{SUR}. Additional deep-infiltration losses (Q_L, a calibration parameter) from S_S represent groundwater export to adjacent catchments. Riparian reservoir S_{UR} receives water from S_F, S_S and rainfall (Table 1, Eq. (13)). Excess water, estimated using a runoff-generation coefficient ($C_{R,R}$), is routed to S_R (R_R). The water that remains in S_{UR} is available for transpiration (E_{UR}, Table 1, Eq. (14)). S_R drains into the stream according to a linear storage-discharge relationship that is controlled by parameter k_R (Table 1, Eq. (18)). The total simulated stream discharge equals the sum of slow and fast contributions from S_S and S_R, respectively (Table 1, Eq. (19)).

https://doi.org/10.5194/hess-2023-292
Preprint. Discussion started: 5 January 2024

Hydrology and Earth System Sciences
Open Access
EGU
Discussions

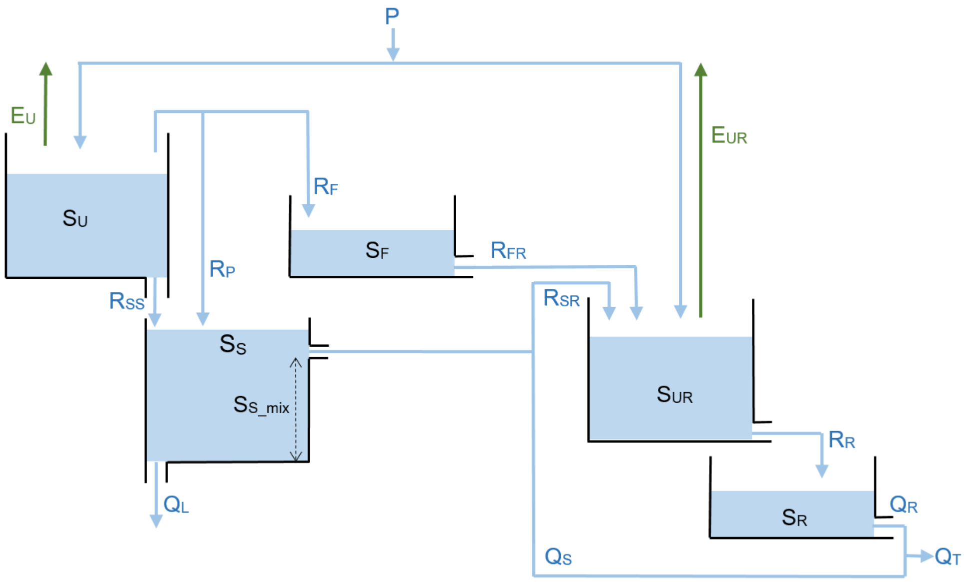

Figure 2. Conceptual model structure used to represent the Kervidy-Naizin catchment. See Table A1 for definitions of the variable abbreviations.

Table 1. State and flux equations of the model. See Table A1 for definitions of the variable abbreviations.

Process	Water balance	Eq.	Flux and state equations, and relationships	Eq.
Unsaturated zone	$dS_U/dt = P - E_U - R_F - R_P - R_{SS}$	(1)	$E_U = E_P min\left(1, \frac{S_U}{S_{U\_max}} \frac{1}{L_P}\right)$	(2)
			$R_U = (1 - C_{H,R})P$	(3)
			$R_F = C_{H,R}(1 - C_P)P$	(4)
			$R_P = C_{H,R} C_P P$	(5)
			$R_{SS} = P_{max}\left(\frac{S_U}{S_{U\_max}}\right)$	(6)
			$C_{H,R} = \frac{1}{\left(1 + exp\left(\frac{-S_U/S_{U\_max} + 0.5}{\beta_H}\right)\right)}$	(7)
Fast reservoir	$dS_F/dt = R_F - R_{FR}$	(8)	$R_{FR} = S_F(1 - e^{-k_F t})dt^{-1}$	(9)
Slow reservoir	$dS_S/dt = (1 - f)(R_{SS} + R_P) - Q_S - R_{SR} - Q_L$	(10)	$Q_S = \begin{cases} (S_S - S_{S\_mix} - Q_L)(1 - e^{-k_S t})dt^{-1} * (1\text{-}f_{SUR}) & ,(S_S - S_{S\_mix} - Q_L) > 0 \\ 0 & ,(S_S - S_{S\_mix} - Q_L) \le 0 \end{cases}$	(11)
			$R_{SR} = \begin{cases} (S_S - S_{S\_mix} - Q_L)(1 - e^{-k_S t})dt^{-1} * f_{SUR} & ,(S_S - S_{S\_mix} - Q_L) > 0 \\ 0 & ,(S_S - S_{S\_mix} - Q_L) \le 0 \end{cases}$	(12)
Riparian unsaturated reservoir	$dS_{UR}/dt = P + \frac{R_{FR}(1 - f)}{f} + \frac{R_{SR}}{f} - E_{UR} - R_R$	(13)	$E_{UR} = E_P min\left(1, \frac{S_{UR}}{S_{UR\_max}} \frac{1}{L_P}\right)$	(14)
			$R_R = C_{R,R} P$	(15)
			$C_{R,R} = min\left(1, \left(\frac{S_{UR}}{S_{UR\_max}}\right)^{\beta_R}\right)$	(16)
Riparian reservoir	$dS_R/dt = R_R - Q_R$	(17)	$Q_R = S_R(1 - e^{-k_R t})dt^{-1}$	(18)
Total runoff	$Q_T = Q_S + fQ_R$	(19)		
Total evaporative fluxes	$E_A = (1 - f)(E_U) + f(E_{UR})$	(20)		

https://doi.org/10.5194/hess-2023-292
Preprint. Discussion started: 5 January 2024

Hydrology and Earth System Sciences
Discussions

2.3.2. Nitrate transfer and transformation

N inputs to reservoirs S_U and S_{UR} are the daily N surplus (kg N ha^{-1}), which correspond to soil N balances. N inputs consist of inorganic and organic fertilisers (i.e. slurry and manure), biological N fixation and atmospheric N deposition. N outputs equal the sum of N exported by each crop type. In this study, the N surplus was considered as a net (N inputs - N outputs) diffuse N source for the catchment (Dupas et al., 2020). Farm surveys performed in 2008 and 2013 led to estimates of a mean annual surplus over the study period (2002–2017) of ca. 90 kg N ha^{-1} y^{-1} (Casal, 2018). Given the uncertainty in the estimated N surplus, we considered it as calibration parameter (surplusN, Table 2).

Biological transformation of NO_3^-, either by denitrification in the riparian zone or by consumption in the stream by aquatic primary producers, was simulated as a constant annual amount of NO_3^- removal (Rc) (kg N ha^{-1} yr^{-1}) in reservoir S_R. The main factors that limit denitrification are NO_3^- availability, temperature, soil moisture and light (Billen et al., 1994; Oehler et al., 2009). These factors vary seasonally and, to some extent, are likely to compensate for each other; for example, in winter, riparian-zone saturation favours anoxic conditions and often higher N concentrations, whereas in summer, temperature and light intensity favour biological activity. Furthermore, even if NO_3^- removal were higher in winter, its effect on NO_3^- concentration would be negligible given the large NO_3^- load. Therefore, representing biological removal as a constant (Rc, Table 2) was assumed to be reasonable in a parsimonious model approach (Fovet et al., 2015b).

2.3.3. Dissolved organic carbon transfer and transformation

The conceptualization of biogeochemical processes used to simulate DOC dynamics, similar to that of Birkel et al. (2014), is based on a simple production-loss mass balance and transport along the main flow pathways to the stream. The DOC mass balance ($\Delta mass_{DOC_i}$ [M]), during a time step Δt [T], of each reservoir i (i.e. S_U, S_{UR} and S_S) differs from more complex carbon process models by being simplified into a grouped representation of DOC production ($Production_{DOC_i}$ [M]) (processes that transform carbon were not distinguished) and loss ($Loss_{DOC_i}$ [M]) (processes that consume, retain, and mineralize DOC were not distinguished) (Koch et al., 2013; Di Grazia et al., 2023). We assumed that in-stream processes have negligible influence on DOC concentrations (Birkel et al., 2014, 2020):

$$\Delta mass_{DOC_i} = Production_{DOC_i} - Loss_{DOC_i} \quad (21)$$

DOC was assumed not to be produced in the groundwater reservoir (S_S) because empirical studies usually find no DOC sources in it (Kalbitz and Kaiser, 2008); however, DOC can accumulate in S_S due to recharge from the hillslope reservoir (S_U). DOC production of reservoir i (i.e. S_U and S_{UR}), during a time step Δt, was assumed to increase as temperature and soil water content increased:

$$Production_{DOC_i} = k_{DOC_i} \frac{S_i}{S_{i\_max}} E_a{}^{T-\overline{T}} * V_i \quad (22)$$

where k_{DOC_i} [M L^{-3}] is the concentration at which DOC is produced daily in a reservoir i, E_A (dimensionless) is a calibrated temperature-dependent activation energy, T [°C] is the observed daily air temperature, $\overline{T}$ [°C] is the mean annual air temperature for the study period, S_{i_max} and S_i the capacity [L] and total water stored [L], respectively, of reservoir i, and V_i the water volume of reservoir i [L^3]. In this study we applied a time step of Δt = 1 day.

https://doi.org/10.5194/hess-2023-292
Preprint. Discussion started: 5 January 2024

Hydrology and Earth System Sciences
Discussions

Potential DOC losses ($Loss_{DOC_i}$ [M]) in the form of mineralization (Köhler et al., 2002), absorption or consumption in reservoirs S_U, S_{UR} and S_S are calculated using a loss coefficient parameter (L_{DOC_i}) (dimensionless, see Table 2) applied to the DOC mass of reservoirs at the beginning of time step.

The daily solute (NO_3^- or DOC) concentration at the outlet ($C_{out_{solute}}$ [M L^{-3}]) is then calculated according to the relative contribution of reservoirs S_S and S_R:

$$C_{out_{solute}} = \frac{C_{solute_{SS}} \cdot Q_S + C_{solute_{SR}} \cdot Q_R}{Q_T} \tag{23}$$

Table 2. Definitions and uniform prior distributions of the parameters of the solute-transport model.

Module	Parameter	Unit	Initial Range	Definition
Rainfall-Runoff	S_{U_max}	[mm]	[50-1000]	Storage capacity of the hillslope unsaturated zone
	C_P	[-]	[0.005-1.0]	Preferential recharge coefficient
	β_H	[-]	[0.01-4]	Hillslope runoff coefficient
	P_{max}	[L T^{-1}]	[0.1-6]	Percolation capacity
	L_P	[-]	[0.01-0.8]	Transpiration threshold
	k_F	[d^{-1}]	[0.001-1]	Storage coefficient of the fast reservoir
	k_S	[d^{-1}]	[0.02-0.06]	Storage coefficient of the slow reservoir
	S_{S_mix}	[mm]	[500-9000]	Groundwater mixing volume in the slow reservoir
	f_{SUR}	[-]	[0.00001-0.2]	Proportion of water flow from reservoir S_S that passes through reservoir S_{UR}
	Q_L	[mm. d^{-1}]	[0.05-1]	Deep infiltration loss
	f	[-]	[0.15-0.30]	Proportion of the catchment covered by the riparian zone
	S_{UR_max}	[mm]	[50,500]	Storage capacity in the riparian unsaturated zone
	β_R	[-]	[1-7]	Riparian runoff coefficient
	k_R	[d^{-1}]	[0.04-2]	Storage coefficient of the riparian reservoir
Nitrate	surplusN	[kg.ha^{-1}.year^{-1}]	[50-95]	Nitrogen surplus
	Rc	[kg.ha^{-1}.year^{-1}]	[25-40]	Amount of nitrate removed
Dissolved organic carbon (DOC)	$k_{DOC_{SU}}$	mg. L^{-1}	[15-35]	DOC concentration rate in unsaturated storage
	$k_{DOC_{SUR}}$	mg. L^{-1}	[15-35]	DOC concentration rate in riparian storage
	E_A	[-]	[1.0-1.2]	Energy parameter
	$L_{DOC_{SU}}$	[-]	[0-1]	DOC loss in unsaturated storage
	$L_{DOC_{SS}}$	[-]	[0-1]	DOC loss in slow storage
	$L_{DOC_{SUR}}$	[-]	[0-1]	DOC loss in riparian storage

2.3.4. Mixing assumption

Each reservoir in the model is assumed to be completely mixed to simulate solute dynamics. This approach, used in most studies based on conceptual models (McMillan et al., 2012; Birkel et al., 2020; Pesántez et al., 2023), assumes instantaneous and complete mixing of the incoming water and solute masses in each reservoir, according to a solute-balance equation:

$$\frac{\mathrm{d}(c_i S_i)}{\mathrm{d}t} = \sum_j c_{I,j} \, I_j - \sum_k c_{O,k} \, O_k \tag{24}$$

where S_i is the amount of water stored in reservoir i [L^3], c_i is the associated solute concentration [M L^{-3}], I are the j water-inflow [L^3 T^{-1}] to a given reservoir (e.g. R_{SS} and R_P from S_U to S_S) (Fig. 2) with the corresponding solute-inflow concentrations $c_{I,j}$ [M L^{-3}], and O are the k water-outflow [L^3 T^{-1}] from a given reservoir with the corresponding solute-outflow concentrations $c_{O,k}$ [M L^{-3}] (e.g. R_{SR} and Q_S from S_S) (Fig. 2).

https://doi.org/10.5194/hess-2023-292
Preprint. Discussion started: 5 January 2024

Hydrology and Earth System Sciences
Open Access
EGU
Discussions

The model tracks the distribution of ages of the water outflow ($p_{Outflow}(T, t)$, where T is the transit time at time t; see Benettin et al., 2022)) using a time stamp for each daily incoming and outflowing water flux in reservoirs, similar to the approach of Birkel and Soulsby (2016). The distribution of ages of water in a reservoir ($p_S(T, t)$) can be derived in a similar way to tracking the ages of water in outflow ($p_{Outflow}(T, t)$), as they are related by a StorAge-Selection (SAS) function developed by Botter et al. (2011):

$$\omega_{Outflow}(T,t) = \frac{p_{Outflow}(T,t)}{p_S(T,t)} \tag{25}$$

The SAS function can be considered a statistical summary of the transport behaviour of a hydrological system that quantifies the release of water of different ages from a reservoir to an outflow (Rinaldo et al., 2015). According to the complete mixing assumption of these model, the age distributions of storage and flux are identical to each other, i.e the outflow composition is perfectly representative of the storage composition (Benettin et al., 2022). Thus, the solute concentration of outflow equals the solute concentration of the reservoir. This “well-mixed” situation corresponds to uniform sampling in which $\omega_{Outflow}(T,t) = 1$ and implies that water storage is uniformly (or randomly) sampled by an outflow (Benettin et al., 2013).

2.4. Sensitivity analysis of the solute-transport model

A global sensitivity analysis (GSA) was carried out to determine the effect of the model calibration scenarios on the most sensitive hydrological parameters. GSA allows to identify the extent to which changes in different parameters influence changes in the hydrological model output, and to determine the most important parameters (i.e. that need to be calibrated) and the least important parameters (i.e. that can be fixed as constants) (Reusser et al., 2011; Wang and Solomatine, 2019). GSA, which ranks the relative influence of model parameters on model output (Sun et al., 2022), is generally recommended for hydrological models due to its advantages over local sensitivity analysis methods, such as its ability to consider the influence of input parameters over their entire range of variation and its suitability for non-linear and non-monotonic models, thus providing results that are independent of modeller bias and a particular site (Song et al., 2015). Among the GSA methods widely applied to hydrological models, we chose a variance-based method as it can provide the most accurate and robust sensitivity indices for complex non-linear models (Reusser et al., 2011; Song et al., 2015; Wang and Solomatine, 2019). Variance-based methods assume that a parameter’s influence can be measured by the contribution of the parameter itself or its interactions with two or more other parameters to the variance of the output. The main advantage of variance-based methods is that they can calculate the main and higher-order effects of parameters, which identifies which ones strongly influence the output on their own, and which ones strongly influence the output due to their interactions with other parameters (Wang and Solomatine, 2019). We used the Fourier Amplitude Sensitivity Test (FAST) (Saltelli et al., 1999) from the SPOTPY Python framework (Houska et al., 2015) to calculate variance-based sensitivity indices that ranged from 0-1. FAST calculates a first-order sensitivity index (S_i), which measures the effect of each parameter on the output, and a total sensitivity index (S_{Ti}), which measures the effect of each parameter and its interactions with the other parameters on the output (Shin and Kim, 2017). Because S_{Ti} provides more reliable results than S_i when investigating the overall influence of each parameter on the output (Saltelli et al., 2009), we used it to investigate parameter sensitivity, as defined by Saltelli and Annoni (2010):

$$S_{Ti} = \frac{E_{X_{\sim i}}\left(V_{X_i}(Y|X_{\sim i})\right)}{V(Y)} \tag{26}$$

where X_i is the i[th] parameter, and $X_{\sim i}$ is the vector of all parameters except X_i.

The variance between parentheses in the numerator denotes that the variance of Y, the value of the scalar objective function, is considered over all possible values of X_i while keeping $X_{\sim i}$ fixed. The expectation operator outside the

https://doi.org/10.5194/hess-2023-292
Preprint. Discussion started: 5 January 2024

Hydrology and Earth System Sciences
Open Access
Discussions

parentheses is considered over all possible values of $X_{\sim i}$, whereas the variance V(Y) in the denominator is the total (unconditioned) variance (Shin and Kim, 2017). The numerator represents the expected variance if all parameters except X_i are fixed (Saltelli and Annoni, 2010).

Calculating S_{Ti} for a single parameter requires n×(p+2) model runs, where n is the sample size and p is the number of parameters (Saltelli, 2002). To determine an appropriate sample size for this GSA, we relied on the experiment of Nossent et al. (2011), in which the sensitivity index did not converge until n = 12,000; thus, with 14 hydrological parameters, we performed 192,000 model runs. In this GSA, the Nash-Sutcliffe model efficiency coefficient (Nash and Sutcliffe, 1970) was used to assess daily streamflow output, as suggested by Nossent et al. (2011).

2.5. Model calibration and evaluation

To limit adverse effects of equifinality and ensure robust posterior parameter distributions to represent processes meaningfully, extensive multi-objective and multi-variable calibration was performed by calibrating hydrological and biogeochemical model predictions simultaneously. The caRamel algorithm (Monteil et al., 2020) used in this approach combines the multi-objective evolutionary annealing-simplex algorithm (Efstratiadis and Koutsoyiannis, 2008) and the non-dominated sorting genetic algorithm II (Reed and Devireddy, 2004). The caRamel algorithm produces an ensemble of parameter sets (i.e. a "generation") to run the model, downscales the generation to the parameter sets that optimize the objective functions and generates a new parameter set that produces more accurate results. The research hypotheses of this study were tested using a stepwise strategy with four model-calibration scenarios based on different combinations of model-performance metrics (Table 3):

- Scenario 1 (S1): only data on streamflow used for calibration, with six metrics used to describe the predicted streamflow signatures
- Scenario 2 (S2): data on streamflow and stream DOC concentration used for calibration, with two metrics including the mean of the metrics in S1 and the Kling–Gupta efficiency (Gupta et al., 2009) used to assess the predicted DOC concentrations
- Scenario 3 (S3): same as S2, but the solute was NO_3^- instead of DOC
- Scenario 4 (S4): data on streamflow and stream DOC and NO_3^- concentrations used for calibration, with three metrics including the mean of the metrics in S1 and the Kling–Gupta efficiency used to assess the predicted DOC and NO_3^- concentrations.

The calibration period was set from 1 Jan 2013 to 1 Sep 2016, while the evaluation period was set from 1 Aug 2008 to 31 Dec 2011, each simulated after 3 years of initialization. These periods, the same as those of Strohmenger et al. (2021), were chosen to be able to compare model performance to two approaches to solute modelling. The hydrological year 2012 was excluded from these periods due to a problem with laboratory analysis of NO_3^- concentrations that year. The uniform prior parameter distributions are based on previous studies of headwater catchments in similar physiographic contexts (Fovet et al., 2015a; Hrachowitz et al., 2015) (Table 2). The prior distribution of storage coefficient k_S had been narrowly constrained based on previous baseflow-recession analysis using a correlation method (Yang et al., 2018). Three prior parameter constraints (Gharari et al., 2014; Hrachowitz et al., 2014) were added to the calibration algorithm to reduce parameter uncertainties: $k_S < k_F$, $k_F < k_R$ and $S_{UR\_max} < S_{U\_max}$.

Up to 70,000 model runs were used for each calibration scenario, with several successive optimizations to confirm reproducibility of the results, as recommended by Monteil et al. (2020). All parameter sets that belonged to the final Pareto fronts (hereafter, "envelope") were retained as feasible solutions for each calibration scenario (Table 3). To illustrate the results for the predicted discharges and solute concentrations, a "best-compromise" set was

https://doi.org/10.5194/hess-2023-292
Preprint. Discussion started: 5 January 2024

selected from the Pareto front that minimised the Euclidean distance to the optimal point in the multi-objective space of each calibration scenario. All simulated discharges and concentrations using all parameter sets of the Pareto front provided information about the uncertainty in the model's output.

In the later evaluation step, observed soil water content and groundwater level measurements were used as independent data to assess the consistency of internal processes of the best-compromise model for each scenario. Soil moisture is a key variable for the energy and water balance at the land surface. It affects the partitioning of solar radiation into latent and sensible heat as well as the partitioning of precipitation into direct runoff and catchment storage (Duethmann et al., 2022). Accurate prediction of soil moisture is thus essential for simulating streamflow, evapotranspiration and percolation (Rajib et al., 2016; Rajat and Athira, 2021) and for constraining the parameters of hydrological models. The role of groundwater in the seasonal and multi-year dynamics of streamflow is also essential: in many temperate catchments, groundwater stores water during wet periods and releases it throughout the year, thus contributing greatly to low flows (Pelletier and Andréassian, 2022). Therefore, the model's representation of processes can be improved by evaluating its ability to reproduce these key variables dynamics.

The data observed for soil water content at Toullo and PG2 were normalized (from 0-1) as a function of their minimum and maximum values over all of the periods studied. All normalized data observed at Toullo station and point PG2 were compared to the normalized simulated water content in the hillslope reservoir (S_U) and riparian reservoir (S_{UR}), respectively. To compare to the observed groundwater level, the simulated groundwater level was estimated from simulated water storage in the groundwater reservoir (S_S) (Seibert, 2000) using the exponential function $z = -e^{A*S_S+B}$, where S_S is water storage in the slow reservoir, and z is the groundwater level. Coefficients A and B were determined by linear regression between the simulated water storage and the observed groundwater level.

Table 3. Signatures for streamflow, dissolved organic carbon (DOC) and nitrate (NO_3^-) and the associated performance metrics used for model calibration scenarios and evaluation. The size of the Pareto front was the number of solutions. NSE: Nash–Sutcliffe model efficiency coefficient, KGE: Kling–Gupta efficiency.

Calibration scenario	Variables/Signatures	Abbreviation	Performance metric	Size of the Pareto front	References
S1: streamflow only	Time series of streamflow	Q	NSE_Q; KGE_Q	280	Nash and Sutcliffe,1970; Gupta et al., 2009
		Log(Q)	NSE_{logQ}		
	Flow duration curve	FDC	NSE_{FDC}		Jothityangkoon et al., 2001
	Runoff ratio	R_{RUNOFF}	R_{RUNOFF}		Yadav et al., 2007
	Volume error	VE	VE_Q		Criss and Winston, 2008
S2: streamflow and DOC	Streamflow	Q	Mean of metrics of S1	180	
	DOC	DOC	KGE_{DOC}		Gupta et al., 2009
S3: streamflow and NO_3^-	Streamflow	Q	Mean of metrics of S1	110	
	NO_3^-	NO_3^-	KGE_{NO3}		Gupta et al., 2009
S4: streamflow, DOC and NO_3^-	Streamflow	Q	Mean of metrics of S1	270	
	DOC	DOC	KGE_{DOC}		Gupta et al., 2009
	NO_3^-	NO_3^-	KGE_{NO3}		Gupta et al., 2009

https://doi.org/10.5194/hess-2023-292
Preprint. Discussion started: 5 January 2024

3. Results

3.1. Global sensitivity analysis of parameter influence on streamflow

The hydrological parameters that influenced predicted streamflow the most were related to recharge (C_P; S_T = 0.59), deep-infiltration losses (Q_L; S_T = 0.25), percolation capacity (P_{max}; S_T = 0.18), storage capacity of the
380 hillslope unsaturated zone (S_{U_max}; S_T = 0.15) and storage coefficient of the fast-responding reservoir in riparian zone reservoir (k_R; S_T = 0.14) (Fig. 3). The strong influence of C_P was logical, as it determines the recharge from S_U to S_S and S_{UR} to S_R (i.e., how water from runoff is redistributed between the riparian zone and groundwater). Parameters related to the area of the riparian zone (f) and the transpiration threshold (L_P) had less influence.

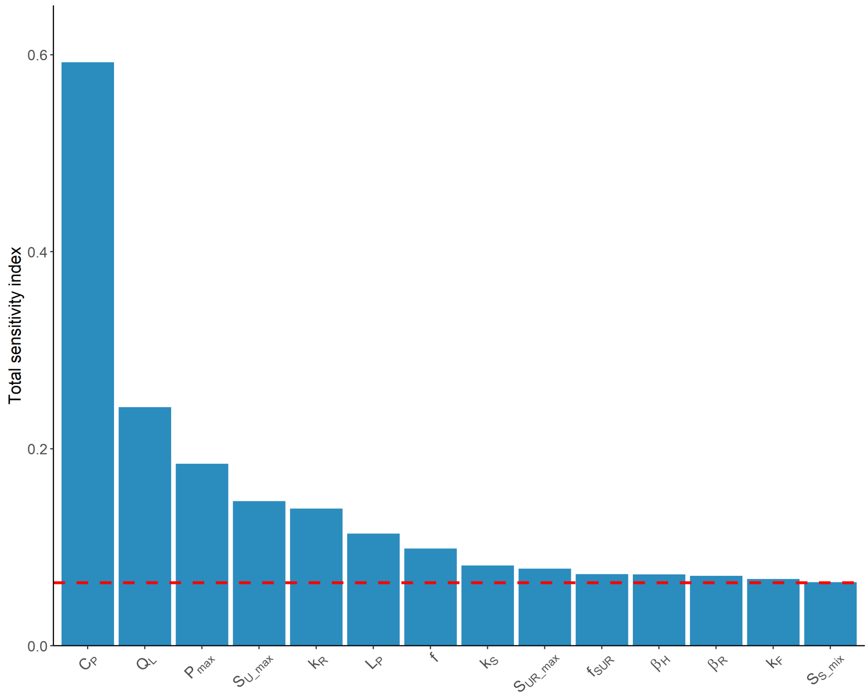

385 **Figure 3**. Total sensitivity indices estimated using the Fourier Amplitude Sensitivity Test of the influence of hydrological parameters on predicted streamflow. The red dashed line represents the minimum total sensitivity index.

3.2. Prediction of streamflow

Overall, the model reproduced the main features of the observed hydrological response (Fig. 4) in both the
390 calibration (NSE_Q, NSE_{logQ} and KGE_Q > 0.8) and evaluation (NSE_Q, NSE_{logQ} and KGE_Q > 0.7) periods for all scenarios. The predicted streamflow reproduced the seasonal dynamics observed during the wetting-up (rising limb of the hydrograph), wet and recession periods. Daily streamflow peaks associated with storm events were reproduced relatively well. Overall, model performances for the evaluation period were only slightly lower than those for the calibration period for all four scenarios. Performance of the best-compromise model was slightly
395 higher for S1 than for the other scenarios, for both calibration and evaluation periods (e.g. comparing S1 (NSE_Q = 0.91, NSE_{logQ} = 0.95, KGE_Q = 0.92) to S4 (NSE_Q = 0.87, NSE_{logQ} = 0.92, KGE_Q = 0.84) for the calibration period)

https://doi.org/10.5194/hess-2023-292
Preprint. Discussion started: 5 January 2024

Hydrology and Earth System Sciences
Open Access
EGU
Discussions

(Fig. 4). The difference in performance between S1 and S2 was smaller. The uncertainty in predicted streamflow estimated from the envelope was low for the calibration and evaluation periods, but appeared to peak during low flow periods. The calibrated model provided similarly reasonable representations of DOC (Fig. 5) and NO_3^- (Fig. 6) concentrations. Predicted DOC concentrations in the calibration period were slightly more accurate for S2 (Fig. 5A) (i.e. KGE_{DOC} = 0.78, $RMSE_{DOC}$= 2.14 mg/l) than for S4 (Fig. 5B) (i.e. KGE_{DOC} = 0.76, $RMSE_{DOC}$ = 2.28 mg/l). Predicted NO_3^-concentrations in the calibration period were slightly more accurate for S3 (Fig. 6A) (i.e. KGE_{NO3} = 0.76, $RMSE_{NO3}$ = 1.87 mg/l) than for S4 (Fig. 6B) (i.e. KGE_{NO3} = 0.74, $RMSE_{NO3}$ = 1.95 mg/l).

The simulated hydrological signatures for all solutions on the Pareto front provide evidence that including solute data in the calibration improves the ability of the model to reproduce certain streamflow characteristics. While the performance based on median hydrological metrics (NSE_Q, NSE_{logQ}, KGE_Q, VE_Q, NSE_{FDC}) was lower overall for S2 and S4 than for S1 for both calibration and evaluation periods (Fig. 7), the median runoff ratio (R_{RUNOFF}) was higher for S4 than for S1 in the evaluation period. In contrast, the performance based on median NSE_Q, NSE_{logQ} and VE_Q metrics was higher for S3 than for S1 for the calibration and evaluation periods. In addition, the runoff ratio (R_{RUNOFF}) was also higher for S3 than for S1 in the evaluation period. These results suggest that simultaneously evaluating model predictions of streamflow and NO_3^- concentration improves the model's ability to reproduce streamflow, especially low flows, due to the improvement in NSE_{logQ}. Compared to S1, the model's hydrological performance decreased the most for S2 and the least for S3. The hydrological metrics for S2 also had wider ranges than those for the other scenarios. Evaluation using DOC concentration showed lower performance for S4 than for S2, while that using NO_3^- concentration showed lower performance for S4 than for S3 (Fig. 7). These results, consistent for both calibration and evaluation periods, supported the observations (Figs. 5 and 6), which suggests that calibrating the model with each solute individually with streamflow better reproduced solute concentrations than calibrating the model with all solutes and streamflow simultaneously.

https://doi.org/10.5194/hess-2023-292
Preprint. Discussion started: 5 January 2024

Hydrology and Earth System Sciences
Open Access
Discussions

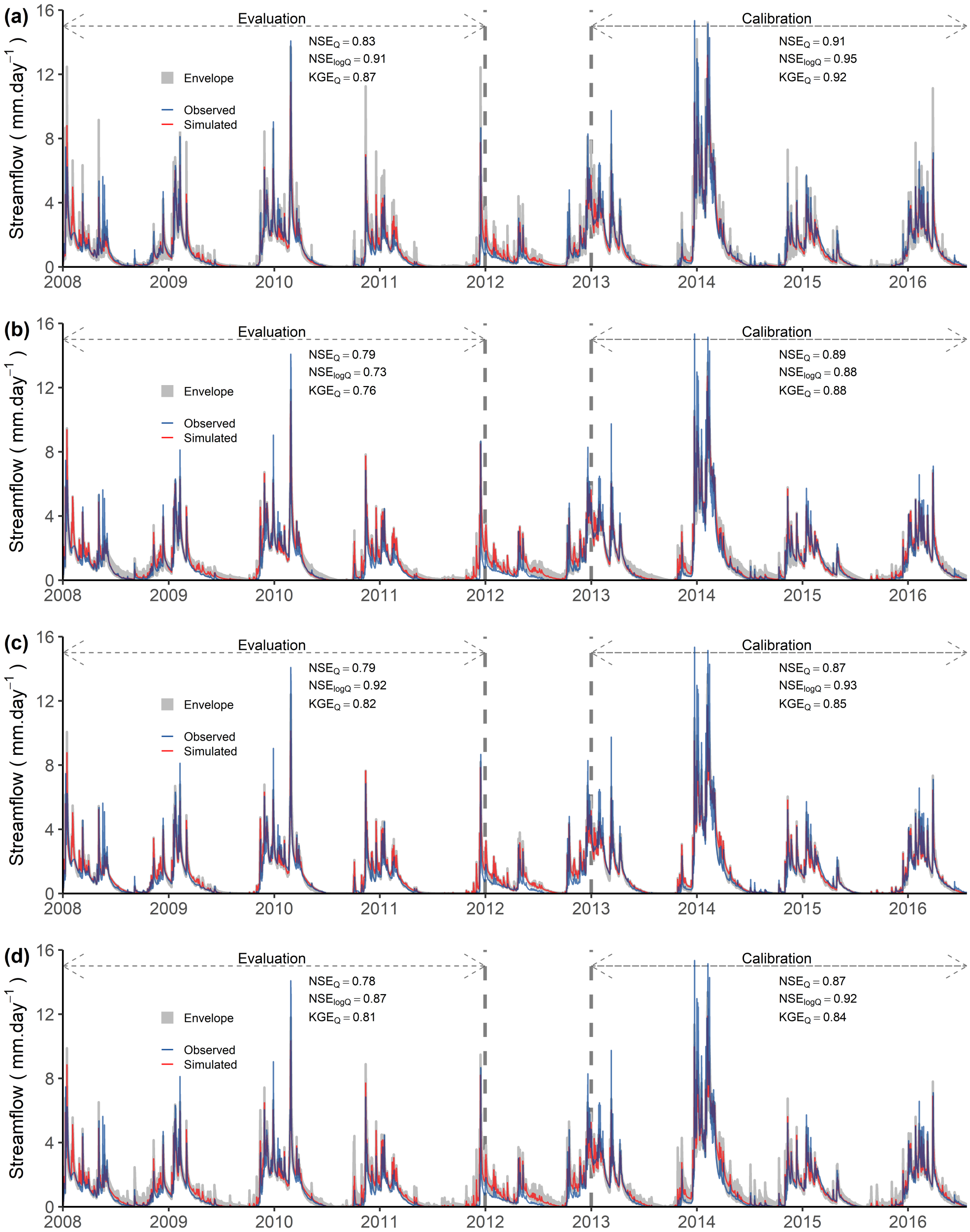

Figure 4. Observed and simulated flows for the calibration and evaluation periods according to the four scenarios: a) S1 (Hydro only), b) S2 (Hydro + dissolved organic carbon (DOC)), c) S3 (Hydro + nitrate (NO_3^-)) and d) S4 (Hydro + DOC + NO_3^-). The simulated data for each scenario correspond to the best-compromise simulated discharge of the set of optimal solutions. "Envelope" refers to the simulated discharge envelope using all parameter sets on the Pareto front. Model-performance metrics are defined in Table 3.

https://doi.org/10.5194/hess-2023-292
Preprint. Discussion started: 5 January 2024

Hydrology and Earth System Sciences
Discussions

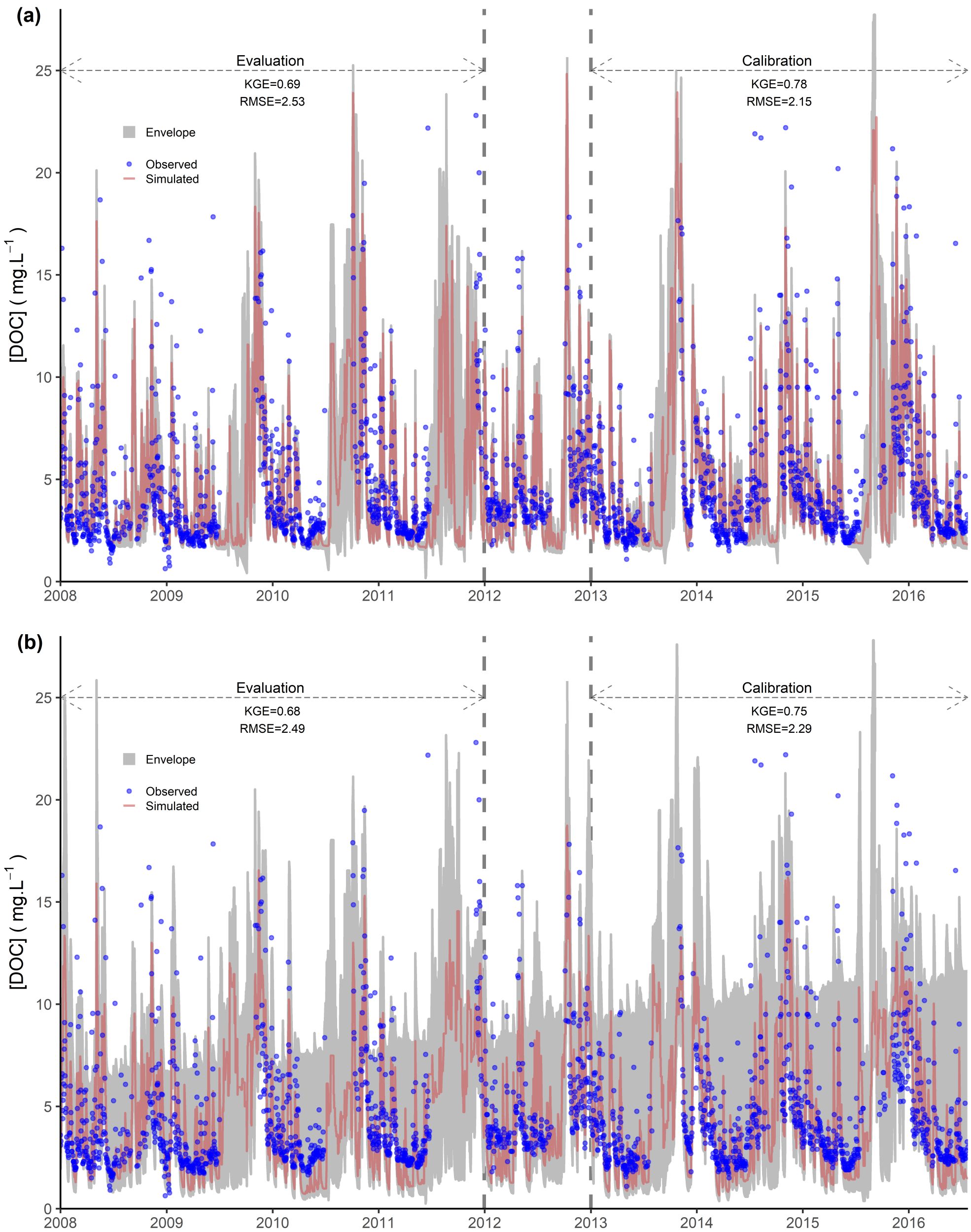

Figure 5. Observed and simulated dissolved organic carbon (DOC) concentrations for the calibration and evaluation periods according to two scenarios: a) S2 (Hydro + DOC) and b) S4 (Hydro + DOC + NO_3^-). The 430 simulated data for each scenario correspond to the best-compromise simulated DOC concentration of the set of optimal solutions. "Envelope" refers to the simulated DOC concentration envelope using all parameter sets on the Pareto front. KGE: Kling–Gupta efficiency, RMSE: Root-mean-square error.

https://doi.org/10.5194/hess-2023-292
Preprint. Discussion started: 5 January 2024

Hydrology and Earth System Sciences
Open Access
Discussions

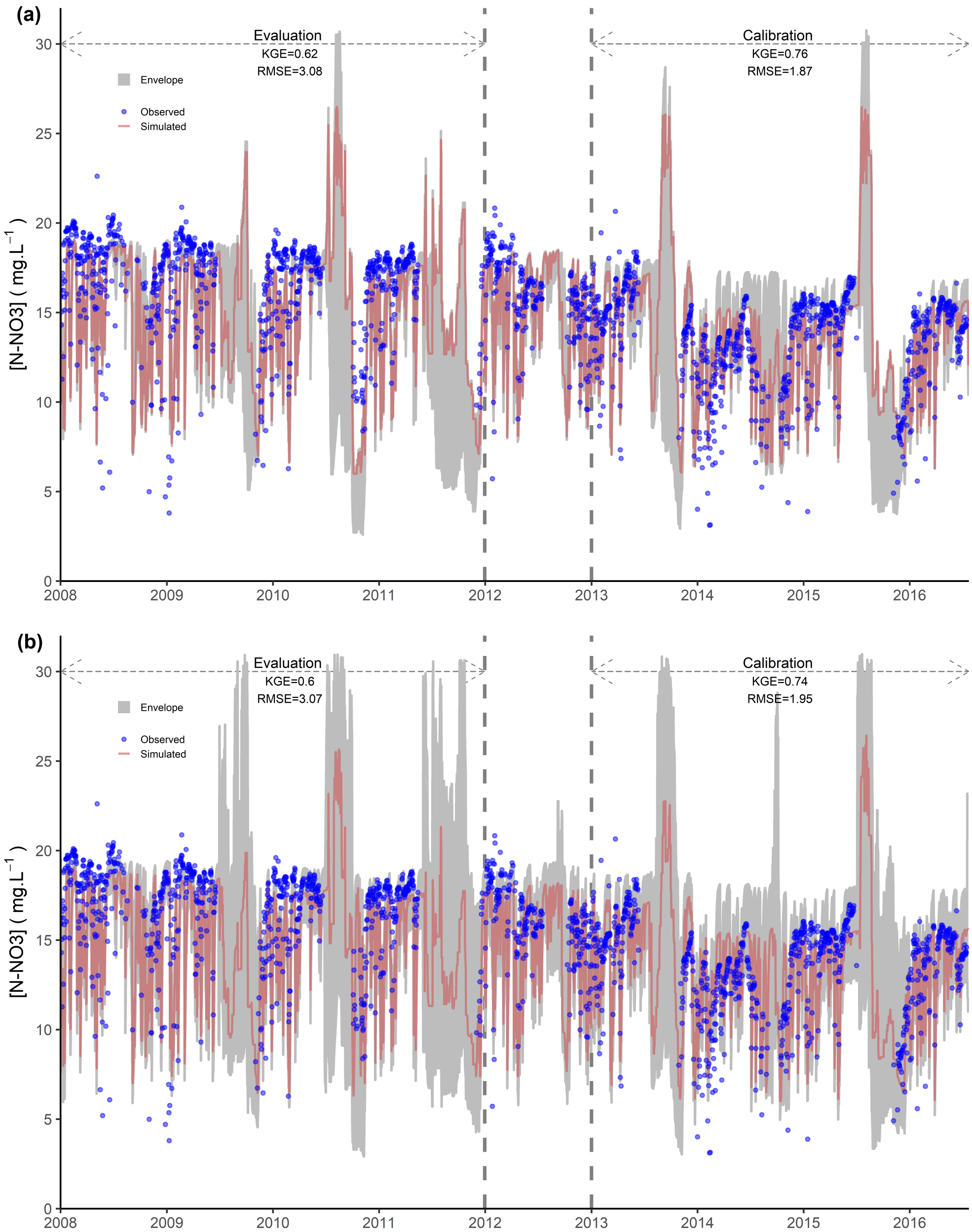

Figure 6. Observed and simulated nitrate (NO_3^-) concentrations for the calibration and evaluation periods according to two scenarios: a) S3 (Hydro + NO_3^-) and b) S4 (Hydro + DOC + NO_3^-). The simulated data for each scenario correspond to the best-compromise simulated NO_3^- concentration of the set of optimal solutions. "Envelope" refers to the simulated NO_3^- concentration envelope using all parameter sets on the Pareto front. KGE: Kling–Gupta efficiency, RMSE: Root-mean-square error.

https://doi.org/10.5194/hess-2023-292
Preprint. Discussion started: 5 January 2024

Hydrology and Earth System Sciences
Discussions
Open Access

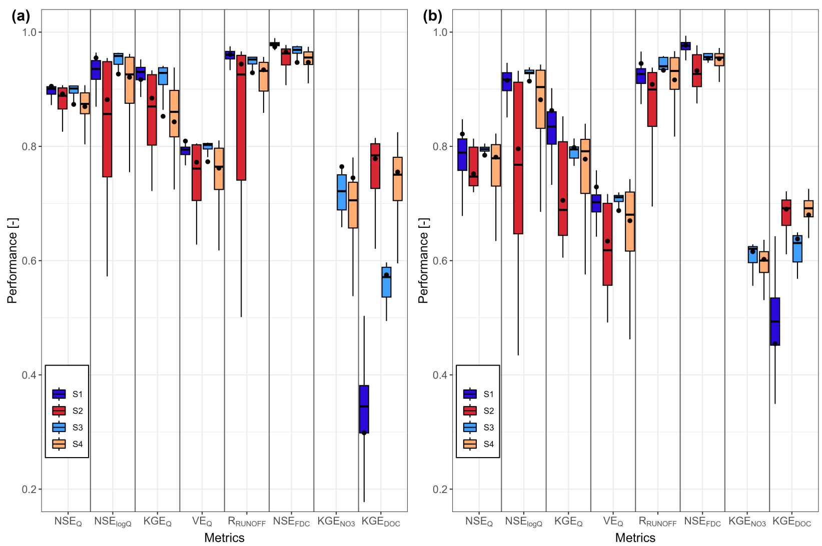

Figure 7. Boxplots of performance metrics for predictions of hydrological and solute concentration according to four scenarios: S1 (Hydro Only), S2 (Hydro + DOC), S3 (Hydro + NO_3^-) and S4 (Hydro + DOC + NO_3^-) for the a) calibration period and b) evaluation period. Whiskers represent 1.5 times the interquartile range. Black circles indicate the best-compromise solution of the Pareto front. The boxplot of KGE_{NO3} for scenarios S1 and S2 are absent because their values were negative.

3.3. Effects on the distribution of hydrological parameters

Overall, the posterior distribution of hydrological parameters differed among the four calibration scenarios (Fig. 8), except for f_{SUR} and k_R, which were less sensitive to the calibration method (i.e. similar optimal values and distributions), indicating that they had been identified well (Fig. 8i, n). For some parameters, the distributions differed only for one scenario, such as S_{U_max} for S3 (Fig. 8a) and P_{max} for S3 (i.e. smaller values and a narrower range of uncertainties) (Fig. 8d). The latter suggests that calibration using NO_3^- concentration strongly influenced soil parameters, decreasing percolation of water from S_U to S_S. Similarly, the distribution of S_{UR_max} for S2 differed from, and had a range of uncertainties narrower than, those of other scenarios, suggesting that calibration using DOC concentration improved identification of S_{UR_max} (Fig. 8l) and that reservoir S_{UR} needs a lower capacity to reproduce both streamflow and DOC concentrations. In addition, for S4, distributions of the most influential hydrological parameters (i.e. C_P and Q_L) (Fig. 8b and 8j), as well as of groundwater parameters k_S, S_{S_mix} and Q_L, differed from those of the other scenarios. Comparing distributions of the groundwater mixing volume in the slow reservoir (S_{S_mix}) for S2 and S3 showed that its size could be decreased by a factor of ca. 3 when calibrating using NO_3^- concentrations instead of DOC concentrations (Fig. 8h). S1 had the lowest values and widest distribution of Lp (Fig. 8e), suggesting that the simulated actual evapotranspiration needed to be lower to reproduce both streamflow and solute concentrations than it did to reproduce streamflow only.

Overall, all parameters except for k_F and k_S had lower uncertainty when the model was calibrated using solute concentrations, whether simultaneously or separately (Fig. 8). More specifically, the uncertainty in β_H, f_{SUR}, β_R and k_R decreased for S2, S3 and S4. The uncertainty in S_{U_max} and C_P decreased only for S2, while that in P_{max} decreased only for S3. For deep-infiltration losses (Q_L), only calibration using DOC and NO_3^- concentrations simultaneously (S4) decreased its uncertainty compared to those for other scenarios (Fig. 8j).

Hydrology and Earth System Sciences
Discussions

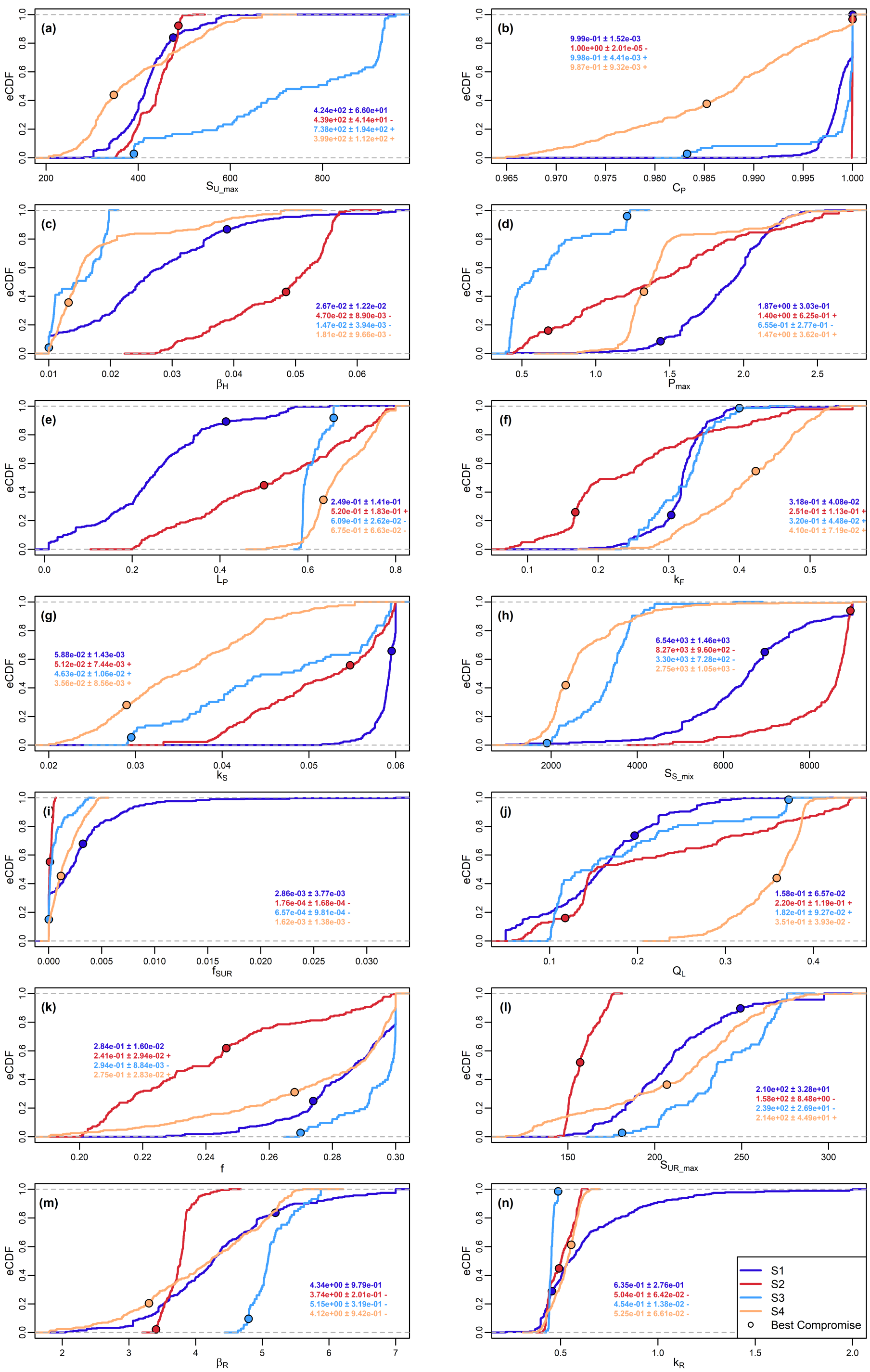

470 **Figure 8**. Posterior cumulative distribution functions of hydrological parameters for the four scenarios: S1 (Hydro Only), S2 (Hydro + DOC), S3 (Hydro + NO_3^-) and S4 (Hydro + DOC + NO_3^-). The circle on each curve indicates

https://doi.org/10.5194/hess-2023-292
Preprint. Discussion started: 5 January 2024

Hydrology and Earth System Sciences
Discussions

the parameter's value in the best-compromise set on the Pareto front for each scenario. Numbers in the graphs show means and standard deviations of each parameter distribution for each scenario. Signs after standard deviations indicate whether the uncertainty in a parameter was lower (-) or higher (+) than that of scenario S1.

3.4. Internal model states and consistency

3.4.1. Groundwater level

The model reproduced the observed magnitude and seasonality of the groundwater level relatively well (NSE = 0.76-0.93, depending on the scenario) (Fig. 9). Low levels of water table were less accurately reproduced in 2009 and 2013. Overall, the calibration that included solute concentrations with streamflow (S2, S3 and S4) greatly improved simulation of groundwater level. In S1, performance metrics NSE and KGE were indeed the lowest, and PBIAS and RMSE were the highest. S3 and S4 reproduced groundwater levels (NSE = 0.92 and 0.93, respectively) better than S2, while S3 reproduced best the low groundwater levels in 2009, 2011 and 2013. However, for S3 and S4, the model tended to slightly overestimate the low groundwater levels in 2010 and 2015.

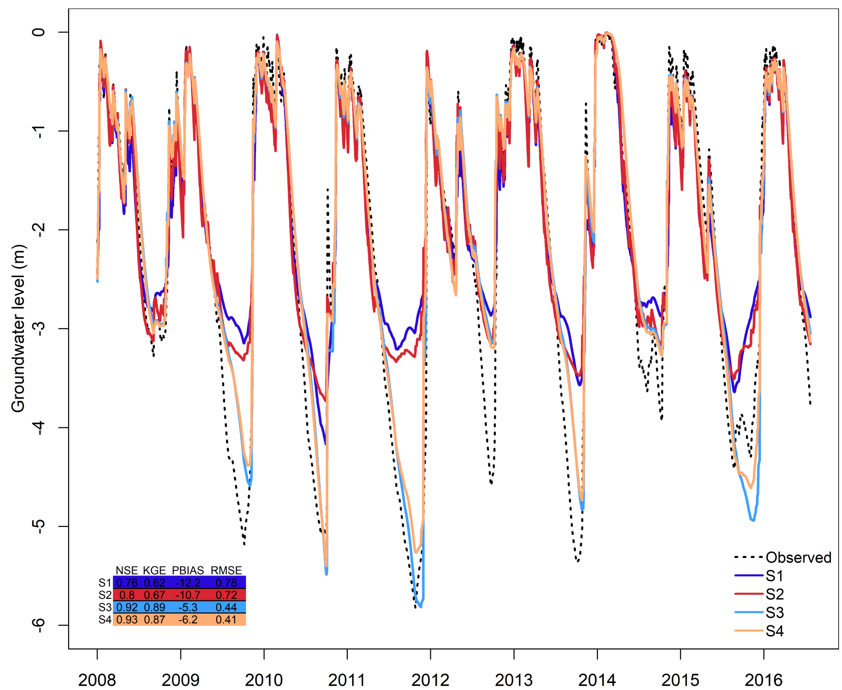

Figure 9. Observed and simulated groundwater levels for the four scenarios: S1 (Hydro Only), S2 (Hydro + DOC), S3 (Hydro + NO_3^-) and S4 (Hydro + DOC + NO_3^-). NSE: Nash–Sutcliffe model efficiency coefficient, KGE: Kling–Gupta efficiency, PBIAS = Percent bias, RMSE: Root-mean-square error.

3.4.2. Soil moisture

The model reproduced major features of the observed dynamics of normalized soil moisture at PG2 (i.e. the riparian zone) (NSE = 0.58-0.79, depending on the scenario) (Fig. 10). It also reproduced well drying rates at the end of summer and wetting rates, except in 2015 and 2016, respectively, when it tended to underestimate soil moisture. Overall, evaluating the model with streamflow and solute concentrations simultaneously did not improve simulation of soil moisture dynamics in the riparian zone. The model reproduced observed soil moisture better

https://doi.org/10.5194/hess-2023-292
Preprint. Discussion started: 5 January 2024

Hydrology and Earth System Sciences
Discussions

when it was calibrated using DOC and NO_3^- simultaneously (S4, with NSE = 0.73 and KGE = 0.78) than when using only one solute (S2 or S3, with NSE = 0.58 and 0.69, respectively, and KGE = 0.74 and 0.75, respectively). The model reproduced the observed dynamics of normalized soil moisture at Toullo (i.e. the upslope zone) (NSE = 0.79-0.92, depending on the scenario) (Fig. 11). For S3 and S4, the model did not reproduce the wetting rate well at the beginning of 2017, when it overestimated soil moisture. S2 reproduced soil moisture in the upslope zone better than S1 did (NSE = 0.94 and 0.92, respectively).

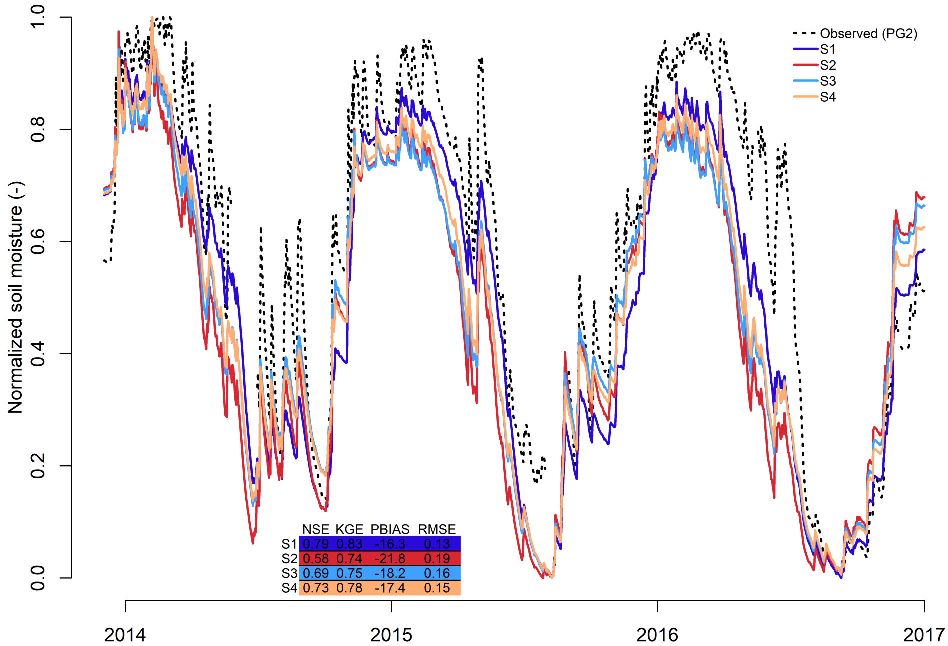

Figure 10. Observed (point PG2) and simulated soil moisture for the for scenarios: S1 (Hydro Only), S2 (Hydro + DOC), S3 (Hydro + NO_3^-), S4 (Hydro + DOC + NO_3^-). NSE: Nash–Sutcliffe model efficiency coefficient, KGE: Kling–Gupta efficiency, PBIAS = Percent bias, RMSE: Root-mean-square error.

https://doi.org/10.5194/hess-2023-292
Preprint. Discussion started: 5 January 2024

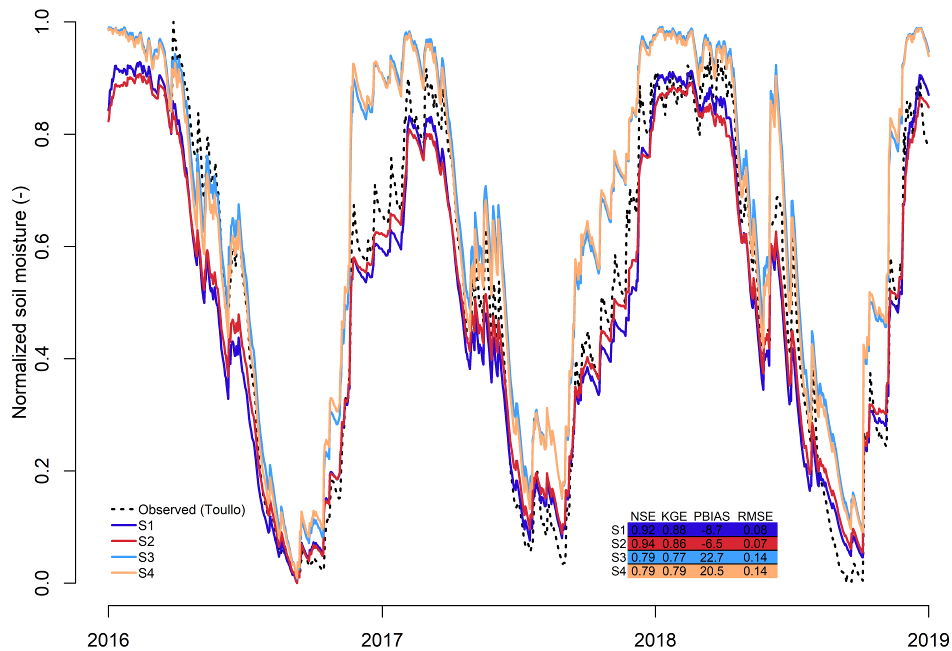

Figure 11. Observed (Toullo point) and simulated normalized soil moisture for four calibration scenarios: S1 (Hydro Only), S2 (Hydro + DOC), S3 (Hydro + NO_3^-), S4 (Hydro + DOC + NO_3^-). NSE: Nash–Sutcliffe model efficiency coefficient, KGE: Kling–Gupta efficiency, PBIAS = Percent bias, RMSE: Root-mean-square error.

3.5. Water balances

Calibrating the model with DOC and NO_3^- concentrations along with streamflow data influenced water-balance components and changed the storage in reservoirs S_U, S_S and S_{UR}. Median simulated total evaporative flux (E_U and E_{UR}) was highest for S1 (470 mm yr^{-1}) and lowest for S4 (372 mm yr^{-1}) (Fig. 12a). Median deep-infiltration losses (Q_L) were highest for S4 (128 mm yr^{-1}) and lowest for S1 (57 mm yr^{-1}). The median contribution of S_R to discharge (Q_R) was slightly higher for S3 and S4 (108 and 109 mm yr^{-1}, respectively) than for S1 (100 mm yr^{-1}). The median contribution of S_S to discharge (Q_S) was significantly higher for S2 (293 mm yr^{-1}) than for S1 (242 mm yr^{-1}). S_S and S_{UR} stored water during the simulation, while S_U lost water. S_S tended store more water for S4 (2.7 mm yr^{-1}) than it did for S1 (1.2 mm yr^{-1}). S_U lost more water for S3 (-21 mm yr^{-1}) than for S1 (-12 mm yr^{-1}) and lost the least for S4 (-10.6 mm yr^{-1}).

https://doi.org/10.5194/hess-2023-292
Preprint. Discussion started: 5 January 2024

Hydrology and Earth System Sciences
Open Access
Discussions

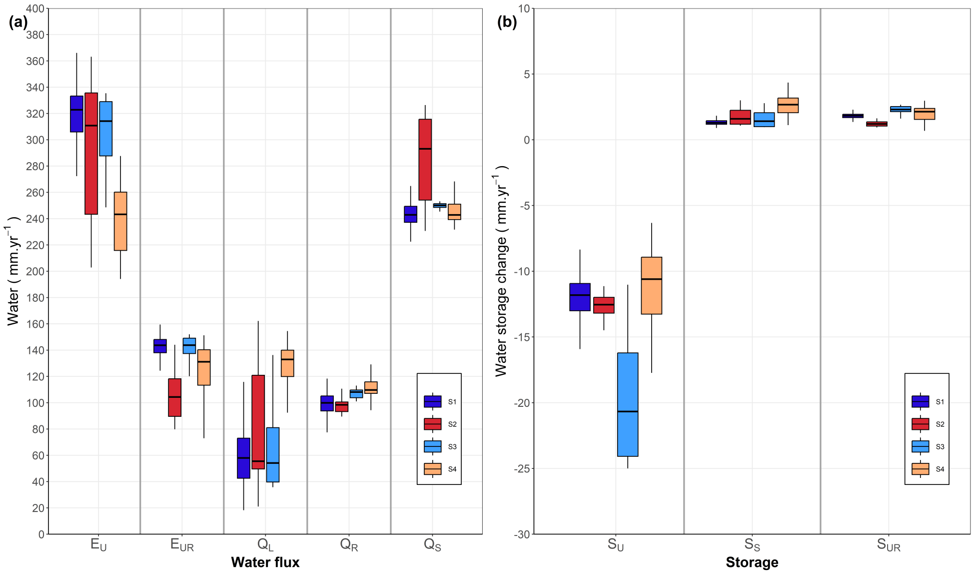

Figure 12. a) Boxplots of simulated annual water budgets for all Pareto fronts of each scenario (S1-S4) during the calibration and evaluation periods combined (1 Aug 2008-1 Sep 2016). Precipitation was 852 mm yr^{-1} during the period. b) Boxplots of changes in simulated storage of the main reservoirs of the model for all Pareto fronts of each scenario during the period. Whiskers represent 1.5 times the interquartile range.

4. Discussion

4.1. Effect on streamflow, groundwater and soil moisture

We found that including solute (DOC and NO_3^-) data along with streamflow data in a multi-objective calibration strategy improved the model's internal consistency, as demonstrated by improved performance for simulations of groundwater storage and soil moisture in the upslope zone (Figs. 9 and 11). Studies have shown that using additional information to constrain hydrological models usually improves spatial and/or temporal patterns of internal state variables and fluxes but does not necessarily improve the accuracy of predicted runoff (López López et al., 2017; Tong et al., 2021). Woodward et al. (2013b) developed a catchment simulation model that predicted streamflow and water chemistry by connecting a model of soil water balance to two groundwater reservoirs. They found that calibrating the model using daily streamflow and monthly NO_3^- data simultaneously from a small lowland milk-production-oriented catchment improved hydrological understanding and estimated catchment NO_3^- fluxes relatively well. In particular, they were able to infer daily contributions of near-surface water, fast shallow groundwater, and slower, deeper groundwater to water and NO_3^- discharge. However, including NO_3^- data in the calibration overpredicted low flows compared to calibration using streamflow data alone. Yen et al. (2014) used regional estimates of annual denitrification mass and the percentage of NO_3^- load at the catchment outlet that had come from groundwater as soft data to constrain water-flow partitioning, which yielded realistic internal catchment behaviour but decreased the accuracy of predicted streamflow. In the present study, when considering only the best-compromise model for each scenario, the use of solute data improved the internal consistency but slightly decreased the accuracy of predicted streamflow in both calibration and evaluation periods (Fig. 4). In contrast, considering all hydrological signatures for discharge obtained from the envelope, S3 improved the model's ability to reproduce streamflow characteristics, especially low flows (Fig. 7) and groundwater level (Fig. 9). In addition, calibrating the model with streamflow and solute concentrations simultaneously improved the internal consistency of the groundwater reservoir, with better reproduction of groundwater level for S3 and S4 (Fig. 9) than that of the soil compartment, with a relatively small improvement in the normalized soil moisture only for S2 in the upslope zone (Fig. 11).

The factors that improve internal hydrological consistency when solute data are included are not well understood. Streamflow aggregates information from many catchment-scale processes, but this information is too ambiguous to determine the exact catchment configuration (Kuppel et al., 2018b) or flow pathways that produced the observed signal (Woodward et al., 2017). This is because streamflow aggregates downstream along a convergent network towards a single outlet, but the divergent nature of an upstream network makes it impossible to uniquely backtrack the locations where the flow was generated (Kirchner et al., 2001). Thus, streamflow can be simulated well with many alternative model parameterizations, whether or not they are physically consistent (Kirchner, 2006). Results of the present study thus suggest that if streamflow alone is used for calibration, the model predicts discharge correctly for the wrong reason, as the internal consistency is not guaranteed. The model thus simulates water pathways and storage dynamics that do not represent those in the actual catchment. Consequently, it appears that the hydrological behaviour of the catchment required to reproduce the observed DOC and NO_3^- concentrations in the stream is different from that required to reproduce only the observed discharge. This hypothesis is supported by the fact that the calibration scenarios influenced the main components of the water balance differently. For example, S3 yielded better internal consistency of the groundwater reservoir, with good reproduction of the groundwater level (Fig. 9), but lower evapotranspiration and higher water loss from the S_U reservoir than S1 (Fig. 12). In comparison, S2 yielded better simulation of upslope soil water storage (Fig. 11) and a higher contribution of S_S to discharge than S1 (Fig. 12). The large amount of information in the solute time series thus constrained internal storage components and water fluxes more than a streamflow-only approach, which increased internal consistency of the hydrological model. This occurs because a hydrological model needs to represent only an input-output response, whereas when biogeochemistry is included, a model needs to represent both residence-time distributions and biogeochemical processing to reproduce the observed stream water concentrations (Medici et al., 2012) and the decrease in solute-input signals. The use of solute time series, which mitigates the equifinality problem, thus excluded infeasible model configurations that would have also yielded high performance (Yen et al., 2014; Kuppel et al., 2018b; Dimitrova-Petrova et al., 2020).

An additional step is needed to understand the benefits of including solute data for internal hydrological consistency by analysing effects of including DOC and NO_3^- concentration data on the storage dynamics (state and fluxes) of model components and hydrological processes and pathways. For example, the simulations showed that including NO_3^- data decreased k_S and S_{S_mix} (Fig. 8g and 8h), suggesting that simulations of NO_3^- dynamics were optimized at a lower groundwater mixing volume and lower flow rate in S_S. However, it is important to go further to understand why including NO_3^- concentration data improved simulation of groundwater level (Fig. 9) and low flow (Fig. 7). In this landscape, most of the NO_3^- leached from the unsaturated reservoir accumulates in the shallow groundwater (Aubert et al., 2013; Strohmenger et al., 2020). The groundwater, with a legacy mass storage of NO_3^- (Molenat et al., 2008; Basu et al., 2010), thus contributes water to the stream that sustains the base flow and export of NO_3^- (Molenat et al., 2008; Aubert et al., 2013). Given these characteristics, good reproduction of NO_3^- concentrations and fluxes in the stream, supplied mainly by groundwater, can be assumed to constrain the model sufficiently to yield good reproduction of water fluxes from the groundwater to the stream and thus good representation of groundwater level.

4.2. Effects on parameter uncertainties

Using a parsimonious hydro-chemical model without explicit biogeochemical processes, Strohmenger et al. (2021) found that overall parameter uncertainties were higher when calibrating using solute data (DOC, NO_3^-) along with streamflow data than when calibrating using streamflow data alone. They assumed that DOC and NO_3^- sources behave as infinite pools with a fixed concentration in each reservoir contributing to the stream. The modelling approach in the present study was relatively similar, but explicitly represented biochemical processes related to DOC and NO_3^-. Parameter uncertainty decreased when solute concentrations were included in calibration, except for storage coefficients of the fast (k_F) and slow reservoirs (k_S) (Fig. 8). Comparing the results of these two studies suggests that the infinite-solute-pool assumption is sufficient to reproduce annual and storm-event dynamics of discharge and DOC and NO_3^- concentrations in the stream but is insufficient to improve the internal consistency or constrain the model to reduce uncertainties in hydrological parameters. In the infinite-solute-pool assumption, hydrological parameters are less sensitive to solute concentrations than they are in models that explicitly represent biogeochemical processes and dynamic solute concentrations in reservoirs. Notably, the results highlight that S4 significantly influenced the distributions of the most influential hydrological parameters, specifically C_P and Q_L (Fig. 8). The model conceptualizes biogeochemical processes for DOC and NO_3^- in a relatively simple way, but has reduced the uncertainties of the parameters. An additional step in future studies will be to analyse whether more complex representation of biogeochemical processes in the model can further reduce uncertainties in hydrological parameters.

Results of the present study are consistent with those of other studies, in which inclusion of additional variables in multiple-objective calibration generally reduced parameter uncertainty (Tong et al., 2021). For example, Yen et al. (2014) found that including data related to water quality yielded lower parameter uncertainties than calibration using streamflow alone, especially for hydrological parameters that strongly influence denitrification. Other studies that included additional data in multi-variable calibration found that it reduced parameter uncertainties. For example, Silvestro et al. (2015) demonstrated that the equifinality of soil parameters was reduced by including satellite-derived soil moisture when calibrating a process-based, spatially distributed hydrological model. Similarly, Rajib et al. (2016) found that including satellite-derived soil moisture, especially that in the rooting zone, reduced parameter uncertainties, particularly for parameters related to subsurface hydrological processes.

4.3. Comparability of point-scale *in-situ* measurements to catchment-scale storage

A remaining issue is the limited comparability of point-scale *in-situ* measurements and simulated soil moisture and groundwater level to catchment-scale storage. In-situ volumetric soil moisture was calculated as the mean of several TDR probes, which reduces uncertainty at the point scale, but upscaling these point measurements to a reservoir that represents a hillslope or riparian zone is associated with uncertainties. Consequently, we considered normalized soil moisture as a proxy for dynamics of unsaturated storage in hillslope and riparian zones (e.g. Hrachowitz et al., 2021). Similarly, we used the daily mean normalized water level at point PG5 as a proxy for groundwater storage dynamics. An additional step in future studies will be to determine how point measurements can be upscaled to areal mean point scale soil moisture and groundwater measurements compatible with catchment-scale storage. A complementary approach is to include other promising methods, such as remote sensing, to estimate the spatial distribution of storage in catchments, especially of soil moisture (Tong et al., 2021; Duethmann et al., 2022). The high spatial resolution, worldwide spatial coverage and increasing availability of remotely sensed data may provide ample opportunities to further constrain hydrological models and their parameters (Nijzink et al., 2018; Bouaziz et al., 2021; Tong et al., 2021; Duethmann et al., 2022; Gomis-Cebolla

https://doi.org/10.5194/hess-2023-292
Preprint. Discussion started: 5 January 2024

et al., 2022). Recent soil moisture data from satellite-derived soil-moisture products (e.g. SMAPL3E, SCATSAR, ASCAT DIREX SWI) with high spatial and temporal resolutions (e.g. 0.5-9.0 km and 1-3 days, respectively) (Duethmann et al., 2022) would help constrain the model of the Kervidy-Naizin catchment. Other promising methods include cosmic-ray neutron-sensor probes to estimate dynamics of near-surface soil water storage (Dimitrova-Petrova et al., 2020) and geodesy and geophysical methods (Fovet et al., 2015a). Additional data can be used to assess the internal representation of evapotranspiration, which has a wide spatial and temporal distribution at the catchment scale, to provide more confidence in simulation of the partitioning of water between soil storage and groundwater recharge (Moazenzadeh and Izady, 2022). For example, using spatially and temporally gridded remotely sensed evapotranspiration data to calibrate the Soil and Water Assessment Tool (SWAT) hydrological model decreased the equifinality of the calibrated parameters compared to calibration using only streamflow data (Shah et al., 2021). These results demonstrate the benefit of using increasingly available open-access remotely sensed evapotranspiration data to improve calibration of hydrological models. These methods provide a spatially aggregated overview of catchment water content and go beyond traditional methods of direct storage observations at the point scale that are limited to a single reservoir (Dimitrova-Petrova et al., 2020).

4.4. Implications

This study's results indicate that solute data are important for improving the internal consistency of hydrological models, which can help guide collection of field data and modelling (Stadnyk and Holmes, 2023). When collecting field data for model calibration, it may be important to collect solute data along with streamflow data. These data can then be used in a hydrological model to which simple representations of biogeochemical processes are added to improve the representation of internal behaviour of the catchment by calibrating streamflow and solutes simultaneously. The type of solute measured is also important, as calibration using NO_3^- improved the internal consistency of the groundwater reservoir, while that using DOC improved the internal consistency of soil water storage in the upslope zone. With the increasing availability of solute data from catchment monitoring, this approach provides an objective way to improve representation of complex hydrological systems when information about their internal functioning is insufficient. A catchment model that represents observed behaviour of the system more accurately can then be used with confidence when assessing scenarios, such as those of nutrient remediation or climate change. If the internal behaviour of the hydrological system is not represented correctly, predicting streamflow acceptably is pointless and perhaps counter-productive, leading to erroneous conclusions and potential mismanagement of catchment resources. For example, Yen et al. (2014) showed that a lack of constraints to realistically represent the internal functioning of a catchment can lead to misleading assessments of pollution-control scenarios, even when typical streamflow performance criteria are satisfied.

https://doi.org/10.5194/hess-2023-292
Preprint. Discussion started: 5 January 2024

Hydrology and Earth System Sciences
Open Access
Discussions

5. Conclusion

The results of this study tend to reject the first hypothesis that using daily stream DOC and NO_3^- concentrations along with streamflow data to calibrate a parsimonious conceptual model improves the model's ability to predict streamflow, as doing so did not improve the model's performance for simulated streamflow in the calibration or evaluation period. In contrast, considering all hydrological signatures for discharge obtained from the envelope, the scenario that included NO_3^- along with streamflow improved the model's ability to reproduce streamflow, especially low flows. The second hypothesis, concerning the improvement of the internal consistency of the model, appeared to be supported for the simulation of groundwater and upslope soil storage, but not for riparian soil storage. For the third hypothesis, explicitly modelling biochemical processes for DOC and NO_3^- reduced the uncertainty in hydrological parameters, except the storage coefficients of the fast and slow reservoirs, compared to an approach in which sources of DOC and NO_3^- were treated as infinite pools with fixed concentrations. The simultaneous inclusion of daily in-stream DOC and NO_3^- concentrations in a parsimonious conceptual model in a multi-objective and multi-variable calibration and evaluation strategy influenced the distribution of the most influential hydrological parameters of the model. Differences among the calibration scenarios also influenced the main components of the water balance. Calibrating the model with streamflow and solute concentrations simultaneously reduced predictions of evapotranspiration. Compared to calibration using streamflow alone, the inclusion of DOC increased the predicted contribution of reservoir S_S to discharge, while the inclusion of NO_3^- increased the predicted loss of water from reservoir S_U. Including the large amount of information in solute time series in hydrological models provided an objective way to improve the representation of complex hydrological systems for which information about internal functioning was insufficient.

Appendix

Table A1. Symbols and definitions of variables in the hydrological model

Symbol	Definition	Symbol	Definition
P	Precipitation [L]	k_F	Storage coefficient of the fast reservoir [T^{-1}]
E_U	Transpiration from S_U [$L\ T^{-1}$]	f	Proportion of the catchment covered by the riparian zone [–]
R_U	Infiltration into the unsaturated reservoir [$L\ T^{-1}$]	Q_S	Runoff from the slow reservoir [$L\ T^{-1}$]
R_F	Recharge of fast reservoir [$L\ T^{-1}$]	R_{SR}	Recharge of S_{UR} from S_S [$L\ T^{-1}$]
R_P	Preferential recharge of the slow reservoir [$L\ T^{-1}$]	Q_L	Deep infiltration loss [$L\ T^{-1}$]
R_{SS}	Recharge of the slow reservoir [$L\ T^{-1}$]	S_S	Storage in the slow reservoir [L]
E_P	Potential evaporation [$L\ T^{-1}$]	S_{S_mix}	Groundwater mixing storage in the slow reservoir [L]
E_A	Actual evaporation [$L\ T^{-1}$]	f_{SUR}	Proportion of water flow from S_S that passes through S_{UR}
S_U	Unsaturated storage [L]	k_S	Storage coefficient of the slow reservoir [T^{-1}]
S_{U_max}	Storage capacity of the hillslope unsaturated zone [L]	E_{UR}	Transpiration from S_{UR} [$L\ T^{-1}$]
L_P	Transpiration threshold [–]	R_R	Recharge of the riparian zone reservoir [$L\ T^{-1}$]
$C_{H,R}$	Hillslope runoff coefficient [–]	$C_{R,R}$	Riparian runoff coefficient [–]
C_P	Preferential recharge coefficient [–]	S_{UR}	Unsaturated storage in the riparian zone [L]
P_{max}	Percolation capacity [$L\ T^{-1}$]	S_{UR_max}	Storage capacity in the riparian unsaturated zone [L]
β_H	Hillslope coefficient [–]	β_R	Riparian coefficient [–]
R_{FR}	Recharge of S_{UR} from S_F [$L\ T^{-1}$]	k_R	Storage coefficient of the riparian zone reservoir [T^{-1}]
S_F	Storage in the fast reservoir [L]	Q_R	Runoff from the riparian zone reservoir [$L\ T^{-1}$]
S_R	Storage in the riparian reservoir [L]	Q_T	Total outflow [$L\ T^{-1}$]

Data availability. The weather data are available obtained from the INRAE CLIMATIK platform (https://agroclim.inrae.fr/climatik/, in French). The hydrochemical data (streamflow, groundwater levels, soil water content, solutes concentrations) are available from the Observatoire de Recherche en Environnement sur les Agro-Hydrosystèmes (ORE AgrHyS) platform (https://www6.inra.fr/ore_agrhys_eng/Data). ORE AgrHyS, funded by INRAE, is part of the OZCAR French Research Infrastructure (https://www.ozcar-ri.org/agrhys-observatory/).

Code availability. The model code is available from https://doi.org/10.5281/zenodo.10161243 or directly from the first author.

Author contributions. All co-authors were involved in the identification of the research questions, conceptualization of the original methods, the interpretation and discussions of the results. JSM implemented the model, performed the simulations, created the figures and prepared the first draft of the manuscript. All co-authors contributed to the content and improvement of the manuscript.

Competing interests. At least one of the (co-)authors is a member of the editorial board of Hydrology and Earth System Sciences.

Acknowledgements. We gratefully acknowledge Chantal Gascuel-Odoux for her insightful comments and suggestions. The authors would like to thank Yannick Hamon and Mikael Faucheux for conducting field and laboratory work, providing essential data for this study. We thank Michelle and Michael Corson for their English and scientific review. This study was performed with the support of the high-performance computing platform MESO@LR at the University of Montpellier.

References

Abbott, B. W., Moatar, F., Gauthier, O., Fovet, O., Antoine, V., and Ragueneau, O.: Trends and seasonality of river nutrients in agricultural catchments: 18years of weekly citizen science in France, Science of The Total Environment, 624, 845–858, https://doi.org/10.1016/j.scitotenv.2017.12.176, 2018.

Adeyeri, O. E., Laux, P., Arnault, J., Lawin, A. E., and Kunstmann, H.: Conceptual hydrological model calibration using multi-objective optimization techniques over the transboundary Komadugu-Yobe basin, Lake Chad Area, West Africa, Journal of Hydrology: Regional Studies, 27, 100655, https://doi.org/10.1016/j.ejrh.2019.100655, 2020.

Aubert, A. H., Gascuel-Odoux, C., Gruau, G., Akkal, N., Faucheux, M., Fauvel, Y., Grimaldi, C., Hamon, Y., Jaffrézic, A., Lecoz-Boutnik, M., Molénat, J., Petitjean, P., Ruiz, L., and Merot, P.: Solute transport dynamics in small, shallow groundwater-dominated agricultural catchments: insights from a high-frequency, multisolute 10 yr-long monitoring study, Hydrol. Earth Syst. Sci., 17, 1379–1391, https://doi.org/10.5194/hess-17-1379-2013, 2013.

Basu, N. B., Destouni, G., Jawitz, J. W., Thompson, S. E., Loukinova, N. V., Darracq, A., Zanardo, S., Yaeger, M., Sivapalan, M., Rinaldo, A., and Rao, P. S. C.: Nutrient loads exported from managed catchments reveal emergent biogeochemical stationarity, Geophysical Research Letters, 37, https://doi.org/10.1029/2010GL045168, 2010.

Benettin, P., van der Velde, Y., van der Zee, S. E. A. T. M., Rinaldo, A., and Botter, G.: Chloride circulation in a lowland catchment and the formulation of transport by travel time distributions, Water Resources Research, 49, 4619–4632, https://doi.org/10.1002/wrcr.20309, 2013.

Benettin, P., Rodriguez, N. B., Sprenger, M., Kim, M., Klaus, J., Harman, C. J., van der Velde, Y., Hrachowitz, M., Botter, G., McGuire, K. J., Kirchner, J. W., Rinaldo, A., and McDonnell, J. J.: Transit Time Estimation in Catchments: Recent Developments and Future Directions, Water Resources Research, 58, e2022WR033096, https://doi.org/10.1029/2022WR033096, 2022.

Bennett, K. E., Cherry, J. E., Balk, B., and Lindsey, S.: Using MODIS estimates of fractional snow cover area to improve streamflow forecasts in interior Alaska, Hydrology and Earth System Sciences, 23, 2439–2459, https://doi.org/10.5194/hess-23-2439-2019, 2019.

Beven, K.: A manifesto for the equifinality thesis, Journal of Hydrology, 320, 18–36, https://doi.org/10.1016/j.jhydrol.2005.07.007, 2006.

Beven, K.: So how much of your error is epistemic? Lessons from Japan and Italy, Hydrological Processes, 27, 1677–1680, https://doi.org/10.1002/hyp.9648, 2013.

Beven, K. and Westerberg, I.: On red herrings and real herrings: disinformation and information in hydrological inference, Hydrological Processes, 25, 1676–1680, https://doi.org/10.1002/hyp.7963, 2011.

Beven, K. J.: Rainfall-runoff modelling: the primer, 2nd ed., Wiley-Blackwell, Chichester, West Sussex ; Hoboken, NJ, 457 pp., 2012.

Billen, G., Garnier, J., and Hanset, P.: Modelling phytoplankton development in whole drainage networks: the RIVERSTRAHLER Model applied to the Seine river system, in: Phytoplankton in Turbid Environments: Rivers and Shallow Lakes: Proceedings of the 9th Workshop of the International Association of Phytoplankton Taxonomy and Ecology (IAP) held in Mont Rigi (Belgium), 10–18 July 1993, edited by: Descy, J.-P., Reynolds, C. S., and Padisák, J., Springer Netherlands, Dordrecht, 119–137, https://doi.org/10.1007/978-94-017-2670-2_11, 1994.

Birkel, C. and Soulsby, C.: Linking tracers, water age and conceptual models to identify dominant runoff processes in a sparsely monitored humid tropical catchment, Hydrological Processes, 30, 4477–4493, https://doi.org/10.1002/hyp.10941, 2016.

Birkel, C., Tetzlaff, D., Dunn, S. M., and Soulsby, C.: Using time domain and geographic source tracers to conceptualize streamflow generation processes in lumped rainfall-runoff models: DUAL-TRACER CONCEPTUALIZED STREAMFLOW GENERATION, Water Resour. Res., 47, https://doi.org/10.1029/2010WR009547, 2011.

Birkel, C., Soulsby, C., and Tetzlaff, D.: Integrating parsimonious models of hydrological connectivity and soil biogeochemistry to simulate stream DOC dynamics: PARSIMONIOUS COUPLED DOC MODEL, J. Geophys. Res. Biogeosci., 119, 1030–1047, https://doi.org/10.1002/2013JG002551, 2014.

Birkel, C., Soulsby, C., and Tetzlaff, D.: Conceptual modelling to assess how the interplay of hydrological connectivity, catchment storage and tracer dynamics controls nonstationary water age estimates, Hydrological Processes, 29, 2956–2969, https://doi.org/10.1002/hyp.10414, 2015.

Birkel, C., Broder, T., and Biester, H.: Nonlinear and threshold-dominated runoff generation controls DOC export in a small peat catchment: NONLINEAR FLOW PATHS CONTROL DOC EXPORT, J. Geophys. Res. Biogeosci., 122, 498–513, https://doi.org/10.1002/2016JG003621, 2017.

Birkel, C., Duvert, C., Correa, A., Munksgaard, N. C., Maher, D. T., and Hutley, L. B.: Tracer-Aided Modeling in the Low-Relief, Wet-Dry Tropics Suggests Water Ages and DOC Export Are Driven by Seasonal Wetlands and Deep Groundwater, Water Resour. Res., 56, https://doi.org/10.1029/2019WR026175, 2020.

Blazkova, S., Beven, K. J., and Kulasova, A.: On constraining TOPMODEL hydrograph simulations using partial saturated area information, Hydrological Processes, 16, 441–458, https://doi.org/10.1002/hyp.331, 2002.

Blöschl, G.: Scaling in hydrology: INVITED COMMENTARY, Hydrol. Process., 15, 709–711, https://doi.org/10.1002/hyp.432, 2001.

Botter, G., Bertuzzo, E., and Rinaldo, A.: Catchment residence and travel time distributions: The master equation: CATCHMENT RESIDENCE TIMES, Geophys. Res. Lett., 38, n/a-n/a, https://doi.org/10.1029/2011GL047666, 2011.

Bouaziz, L., Weerts, A., Schellekens, J., Sprokkereef, E., Stam, J., Savenije, H., and Hrachowitz, M.: Redressing the balance: quantifying net intercatchment groundwater flows, Hydrol. Earth Syst. Sci., 22, 6415–6434, https://doi.org/10.5194/hess-22-6415-2018, 2018.

Bouaziz, L. J. E., Fenicia, F., Thirel, G., de Boer-Euser, T., Buitink, J., Brauer, C. C., De Niel, J., Dewals, B. J., Drogue, G., Grelier, B., Melsen, L. A., Moustakas, S., Nossent, J., Pereira, F., Sprokkereef, E., Stam, J., Weerts, A. H., Willems, P., Savenije, H. H. G., and Hrachowitz, M.: Behind the scenes of streamflow model performance, Hydrol. Earth Syst. Sci., 25, 1069–1095, https://doi.org/10.5194/hess-25-1069-2021, 2021.

Brocca, L., Melone, F., Moramarco, T., Wagner, W., and Hasenauer, S.: ASCAT soil wetness index validation through in situ and modeled soil moisture data in central Italy, Remote Sensing of Environment, 114, 2745–2755, https://doi.org/10.1016/j.rse.2010.06.009, 2010.

Capell, R., Tetzlaff, D., and Soulsby, C.: Can time domain and source area tracers reduce uncertainty in rainfall-runoff models in larger heterogeneous catchments?, Water Resour. Res., 48, 2011WR011543, https://doi.org/10.1029/2011WR011543, 2012.

Hydrology and Earth System Sciences
Open Access
EGU
Discussions

Carluer, N.: Vers une modélisation hydrologique adaptée à l'évaluation des pollutions diffuses : prise en compte du réseau anthropique. Adaptation au bassin versant de Naizin (Morbihan), phdthesis, Doctorat Sciences de la terre, Université Pierre et Marie Curie Paris, 1998.

Casal, L.: Evaluation de scénarios de gestion paysagère de l'azote par modélisation en bassins versants agricoles, These de doctorat, Rennes, Agrocampus Ouest, 2018.

Casal, L., Durand, P., Akkal-Corfini, N., Benhamou, C., Laurent, F., Salmon-Monviola, J., and Vertès, F.: Optimal location of set-aside areas to reduce nitrogen pollution: a modelling study, The Journal of Agricultural Science, 156, 1090–1102, https://doi.org/10.1017/S0021859618001144, 2018.

Casal, L., Durand, P., Akkal-Corfini, N., Benhamou, C., Laurent, F., Salmon-Monviola, J., Ferrant, S., Probst, A., Probst, J.-L., and Vertès, F.: Reduction of stream nitrate concentrations by land management in contrasted landscapes, Nutr Cycl Agroecosyst, 114, 1–17, https://doi.org/10.1007/s10705-019-09985-0, 2019.

Clark, M. P., Kavetski, D., and Fenicia, F.: Pursuing the method of multiple working hypotheses for hydrological modeling: HYPOTHESIS TESTING IN HYDROLOGY, Water Resour. Res., 47, https://doi.org/10.1029/2010WR009827, 2011.

Clark, M. P., Schaefli, B., Schymanski, S. J., Samaniego, L., Luce, C. H., Jackson, B. M., Freer, J. E., Arnold, J. R., Moore, R. D., Istanbulluoglu, E., and Ceola, S.: Improving the theoretical underpinnings of process-based hydrologic models, Water Resources Research, 52, 2350–2365, https://doi.org/10.1002/2015WR017910, 2016.

Criss, R. E. and Winston, W. E.: Do Nash values have value? Discussion and alternate proposals, Hydrological Processes, 22, 2723–2725, https://doi.org/10.1002/hyp.7072, 2008.

Demirel, M. C., Mai, J., Mendiguren, G., Koch, J., Samaniego, L., and Stisen, S.: Combining satellite data and appropriate objective functions for improved spatial pattern performance of a distributed hydrologic model, Hydrology and Earth System Sciences, 22, 1299–1315, https://doi.org/10.5194/hess-22-1299-2018, 2018.

Di Grazia, F., Garcia, X., Acuña, V., Llanos-Paez, O., Galgani, L., Gumiero, B., and Loiselle, S. A.: Modeling dissolved and particulate organic carbon dynamics at basin and sub-basin scales, Science of The Total Environment, 884, 163840, https://doi.org/10.1016/j.scitotenv.2023.163840, 2023.

Dick, J. J., Tetzlaff, D., Birkel, C., and Soulsby, C.: Modelling landscape controls on dissolved organic carbon sources and fluxes to streams, Biogeochemistry, 122, 361–374, https://doi.org/10.1007/s10533-014-0046-3, 2015.

Dimitrova-Petrova, K., Geris, J., Wilkinson, M. E., Rosolem, R., Verrot, L., Lilly, A., and Soulsby, C.: Opportunities and challenges in using catchment-scale storage estimates from cosmic ray neutron sensors for rainfall-runoff modelling, Journal of Hydrology, 586, 124878, https://doi.org/10.1016/j.jhydrol.2020.124878, 2020.

Duethmann, D., Smith, A., Soulsby, C., Kleine, L., Wagner, W., Hahn, S., and Tetzlaff, D.: Evaluating satellite-derived soil moisture data for improving the internal consistency of process-based ecohydrological modelling, Journal of Hydrology, 128462, https://doi.org/10.1016/j.jhydrol.2022.128462, 2022.

Dupas, R., Ehrhardt, S., Musolff, A., Fovet, O., and Durand, P.: Long-term nitrogen retention and transit time distribution in agricultural catchments in western France, Environ. Res. Lett., 15, 115011, https://doi.org/10.1088/1748-9326/abbe47, 2020.

Efstratiadis, A. and Koutsoyiannis, D.: Fitting Hydrological Models on Multiple Responses Using the Multiobjective Evolutionary Annealing-Simplex Approach, in: Practical Hydroinformatics: Computational Intelligence and Technological Developments in Water Applications, edited by: Abrahart, R. J., See, L. M., and Solomatine, D. P., Springer, Berlin, Heidelberg, 259–273, https://doi.org/10.1007/978-3-540-79881-1_19, 2008.

Efstratiadis, A. and Koutsoyiannis, D.: One decade of multi-objective calibration approaches in hydrological modelling: a review, Hydrological Sciences Journal, 55, 58–78, https://doi.org/10.1080/02626660903526292, 2010.

Euser, T., Winsemius, H. C., Hrachowitz, M., Fenicia, F., Uhlenbrook, S., and Savenije, H. H. G.: A framework to assess the realism of model structures using hydrological signatures, Hydrol. Earth Syst. Sci., 17, 1893–1912, https://doi.org/10.5194/hess-17-1893-2013, 2013.

Hydrology and Earth System Sciences
Open Access
EGU
Discussions

Euser, T., Hrachowitz, M., Winsemius, H. C., and Savenije, H. H. G.: The effect of forcing and landscape distribution on performance and consistency of model structures: DISTRIBUTION OF FORCING AND MODEL STRUCTURES, Hydrol. Process., 29, 3727–3743, https://doi.org/10.1002/hyp.10445, 2015.

Fenicia, F., Savenije, H. H. G., Matgen, P., and Pfister, L.: Understanding catchment behavior through stepwise model concept improvement: CATCHMENT BEHAVIOR THROUGH STEPWISE MODEL, Water Resour. Res., 44, https://doi.org/10.1029/2006WR005563, 2008.

Fenicia, F., Kavetski, D., Reichert, P., and Albert, C.: Signature-Domain Calibration of Hydrological Models Using Approximate Bayesian Computation: Empirical Analysis of Fundamental Properties, Water Resources Research, 54, 3958–3987, https://doi.org/10.1002/2017WR021616, 2018.

Fovet, O., Ruiz, L., Hrachowitz, M., Faucheux, M., and Gascuel-Odoux, C.: Hydrological hysteresis and its value for assessing process consistency in catchment conceptual models, Hydrol. Earth Syst. Sci., 19, 105–123, https://doi.org/10.5194/hess-19-105-2015, 2015a.

Fovet, O., Ruiz, L., Faucheux, M., Molénat, J., Sekhar, M., Vertès, F., Aquilina, L., Gascuel-Odoux, C., and Durand, P.: Using long time series of agricultural-derived nitrates for estimating catchment transit times, Journal of Hydrology, 522, 603–617, https://doi.org/10.1016/j.jhydrol.2015.01.030, 2015b.

Fovet, O., Humbert, G., Dupas, R., Gascuel-Odoux, C., Gruau, G., Jaffrezic, A., Thelusma, G., Faucheux, M., Gilliet, N., Hamon, Y., and Grimaldi, C.: Seasonal variability of stream water quality response to storm events captured using high-frequency and multi-parameter data, Journal of Hydrology, 559, 282–293, https://doi.org/10.1016/j.jhydrol.2018.02.040, 2018.

Franks, S. W., Gineste, P., Beven, K. J., and Merot, P.: On constraining the predictions of a distributed model: The incorporation of fuzzy estimates of saturated areas into the calibration process, Water Resources Research, 34, 787–797, https://doi.org/10.1029/97WR03041, 1998.

Freer, J. E., McMillan, H., McDonnell, J. J., and Beven, K. J.: Constraining dynamic TOPMODEL responses for imprecise water table information using fuzzy rule based performance measures, Journal of Hydrology, 291, 254–277, https://doi.org/10.1016/j.jhydrol.2003.12.037, 2004.

Gao, H., Ding, Y., Zhao, Q., Hrachowitz, M., and Savenije, H. H. G.: The importance of aspect for modelling the hydrological response in a glacier catchment in Central Asia, Hydrological Processes, 31, 2842–2859, https://doi.org/10.1002/hyp.11224, 2017.

Gharari, S., Hrachowitz, M., Fenicia, F., Gao, H., and Savenije, H. H. G.: Using expert knowledge to increase realism in environmental system models can dramatically reduce the need for calibration, Hydrol. Earth Syst. Sci., 18, 4839–4859, https://doi.org/10.5194/hess-18-4839-2014, 2014.

Giustolisi, O. and Simeone, V.: Optimal design of artificial neural networks by a multi-objective strategy: groundwater level predictions, Hydrological Sciences Journal, 51, 502–523, https://doi.org/10.1623/hysj.51.3.502, 2006.

Gomis-Cebolla, J., Garcia-Arias, A., Perpinyà-Vallès, M., and Francés, F.: Evaluation of Sentinel-1, SMAP and SMOS surface soil moisture products for distributed eco-hydrological modelling in Mediterranean forest basins, Journal of Hydrology, 608, 127569, https://doi.org/10.1016/j.jhydrol.2022.127569, 2022.

Guillaume, J. H. A., Jakeman, J. D., Marsili-Libelli, S., Asher, M., Brunner, P., Croke, B., Hill, M. C., Jakeman, A. J., Keesman, K. J., Razavi, S., and Stigter, J. D.: Introductory overview of identifiability analysis: A guide to evaluating whether you have the right type of data for your modeling purpose, Environmental Modelling & Software, 119, 418–432, https://doi.org/10.1016/j.envsoft.2019.07.007, 2019.

Güntner, A., Uhlenbrook, S., Seibert, J., and Leibundgut, Ch.: Multi-criterial validation of TOPMODEL in a mountainous catchment, Hydrological Processes, 13, 1603–1620, https://doi.org/10.1002/(SICI)1099-1085(19990815)13:11<1603::AID-HYP830>3.0.CO;2-K, 1999.

Gupta, H. V., Kling, H., Yilmaz, K. K., and Martinez, G. F.: Decomposition of the mean squared error and NSE performance criteria: Implications for improving hydrological modelling, Journal of Hydrology, 377, 80–91, https://doi.org/10.1016/j.jhydrol.2009.08.003, 2009.

Gupta, H. V., Clark, M. P., Vrugt, J. A., Abramowitz, G., and Ye, M.: Towards a comprehensive assessment of model structural adequacy: ASSESSMENT OF MODEL STRUCTURAL ADEQUACY, Water Resour. Res., 48, https://doi.org/10.1029/2011WR011044, 2012.

Hartmann, A., Wagener, T., Rimmer, A., Lange, J., Brielmann, H., and Weiler, M.: Testing the realism of model structures to identify karst system processes using water quality and quantity signatures: KARST SYSTEM IDENTIFICATION, Water Resour. Res., 49, 3345–3358, https://doi.org/10.1002/wrcr.20229, 2013.

Hartmann, G. and Bárdossy, A.: Investigation of the transferability of hydrological models and a method to improve model calibration, Adv. Geosci., 5, 83–87, https://doi.org/10.5194/adgeo-5-83-2005, 2005.

Houska, T., Kraft, P., Chamorro-Chavez, A., and Breuer, L.: SPOTting Model Parameters Using a Ready-Made Python Package, PLoS ONE, 10, e0145180, https://doi.org/10.1371/journal.pone.0145180, 2015.

Hrachowitz, M. and Clark, M. P.: HESS Opinions: The complementary merits of competing modelling philosophies in hydrology, Hydrology and Earth System Sciences, 21, 3953–3973, https://doi.org/10.5194/hess-21-3953-2017, 2017.

Hrachowitz, M., Soulsby, C., Tetzlaff, D., and Malcolm, I. A.: Sensitivity of mean transit time estimates to model conditioning and data availability, Hydrol. Process., 25, 980–990, https://doi.org/10.1002/hyp.7922, 2011.

Hrachowitz, M., Savenije, H., Bogaard, T. A., Tetzlaff, D., and Soulsby, C.: What can flux tracking teach us about water age distribution patterns and their temporal dynamics?, Hydrol. Earth Syst. Sci., 17, 533–564, https://doi.org/10.5194/hess-17-533-2013, 2013.

Hrachowitz, M., Fovet, O., Ruiz, L., Euser, T., Gharari, S., Nijzink, R., Freer, J., Savenije, H. H. G., and Gascuel-Odoux, C.: Process consistency in models: The importance of system signatures, expert knowledge, and process complexity, Water Resour. Res., 50, 7445–7469, https://doi.org/10.1002/2014WR015484, 2014.

Hrachowitz, M., Fovet, O., Ruiz, L., and Savenije, H. H. G.: Transit time distributions, legacy contamination and variability in biogeochemical $1/f^{\alpha}$ scaling: how are hydrological response dynamics linked to water quality at the catchment scale?: How are Hydrological Response Dynamics Linked to Water Quality?, Hydrol. Process., 29, 5241–5256, https://doi.org/10.1002/hyp.10546, 2015.

Hrachowitz, M., Benettin, P., van Breukelen, B. M., Fovet, O., Howden, N. J. K., Ruiz, L., van der Velde, Y., and Wade, A. J.: Transit times-the link between hydrology and water quality at the catchment scale: Linking hydrology and transit times, WIREs Water, 3, 629–657, https://doi.org/10.1002/wat2.1155, 2016.

Hrachowitz, M., Stockinger, M., Coenders-Gerrits, M., van der Ent, R., Bogena, H., Lücke, A., and Stumpp, C.: Reduction of vegetation-accessible water storage capacity after deforestation affects catchment travel time distributions and increases young water fractions in a headwater catchment, Hydrology and Earth System Sciences, 25, 4887–4915, https://doi.org/10.5194/hess-25-4887-2021, 2021.

Huang, Y. and Bardossy, A.: Impacts of Data Quantity and Quality on Model Calibration: Implications for Model Parameterization in Data-Scarce Catchments, Water, 12, 2352, https://doi.org/10.3390/w12092352, 2020.

Hulsman, P., Winsemius, H. C., Michailovsky, C. I., Savenije, H. H. G., and Hrachowitz, M.: Using altimetry observations combined with GRACE to select parameter sets of a hydrological model in a data-scarce region, Hydrology and Earth System Sciences, 24, 3331–3359, https://doi.org/10.5194/hess-24-3331-2020, 2020.

Humbert, G., Jaffrezic, A., Fovet, O., Gruau, G., and Durand, P.: Dry-season length and runoff control annual variability in stream DOC dynamics in a small, shallow groundwater-dominated agricultural watershed, Water Resour. Res., 51, 7860–7877, https://doi.org/10.1002/2015WR017336, 2015.

ISO, E.: 10304-1. Water quality–Determination of dissolved fluoride, chloride, nitrite, orthophosphate, bromide, nitrate and sulfate ions, using liquid chromatography of ions–Part 1: Method for water with low contamination, 33, 1995.

Jothityangkoon, C., Sivapalan, M., and Farmer, D. L.: Process controls of water balance variability in a large semi-arid catchment: downward approach to hydrological model development, Journal of Hydrology, 254, 174–198, https://doi.org/10.1016/S0022-1694(01)00496-6, 2001.

Kalbitz, K. and Kaiser, K.: Contribution of dissolved organic matter to carbon storage in forest mineral soils, Journal of Plant Nutrition and Soil Science, 171, 52–60, https://doi.org/10.1002/jpln.200700043, 2008.

Kirchner, J. W.: Getting the right answers for the right reasons: Linking measurements, analyses, and models to advance the science of hydrology: GETTING THE RIGHT ANSWERS FOR THE RIGHT REASONS, Water Resour. Res., 42, https://doi.org/10.1029/2005WR004362, 2006.

Kirchner, J. W., Feng, X., and Neal, C.: Catchment-scale advection and dispersion as a mechanism for fractal scaling in stream tracer concentrations, Journal of Hydrology, 254, 82–101, https://doi.org/10.1016/S0022-1694(01)00487-5, 2001.

Koch, J. C., Runkel, R. L., Striegl, R., and McKnight, D. M.: Hydrologic controls on the transport and cycling of carbon and nitrogen in a boreal catchment underlain by continuous permafrost, Journal of Geophysical Research: Biogeosciences, 118, 698–712, https://doi.org/10.1002/jgrg.20058, 2013.

Köhler, S., Buffam, I., Jonsson, A., and Bishop, K.: Photochemical and microbial processing of stream and soil water dissolved organic matter in a boreal forested catchment in northern Sweden, Aquat. Sci., 64, 269–281, https://doi.org/10.1007/s00027-002-8071-z, 2002.

Kreye, P., Gelleszun, M., and Meon, G.: Parameter identification in hydrological models using groundwater-level measurements and satellite-based soil moisture, Hydrological Sciences Journal, 64, 633–652, https://doi.org/10.1080/02626667.2019.1599120, 2019.

Kunnath-Poovakka, A., Ryu, D., Renzullo, L. J., and George, B.: The efficacy of calibrating hydrologic model using remotely sensed evapotranspiration and soil moisture for streamflow prediction, Journal of Hydrology, 535, 509–524, https://doi.org/10.1016/j.jhydrol.2016.02.018, 2016.

Kuppel, S., Tetzlaff, D., Maneta, M. P., and Soulsby, C.: EcH_2O-iso 1.0: water isotopes and age tracking in a process-based, distributed ecohydrological model, Geoscientific Model Development, 11, 3045–3069, https://doi.org/10.5194/gmd-11-3045-2018, 2018a.

Kuppel, S., Tetzlaff, D., Maneta, M. P., and Soulsby, C.: What can we learn from multi-data calibration of a process-based ecohydrological model?, Environmental Modelling & Software, 101, 301–316, https://doi.org/10.1016/j.envsoft.2018.01.001, 2018b.

Lan, T., Lin, K., Xu, C.-Y., Tan, X., and Chen, X.: Dynamics of hydrological-model parameters: mechanisms, problems and solutions, Hydrol. Earth Syst. Sci., 24, 1347–1366, https://doi.org/10.5194/hess-24-1347-2020, 2020.

López López, P., Sutanudjaja, E. H., Schellekens, J., Sterk, G., and Bierkens, M. F. P.: Calibration of a large-scale hydrological model using satellite-based soil moisture and evapotranspiration products, Hydrology and Earth System Sciences, 21, 3125–3144, https://doi.org/10.5194/hess-21-3125-2017, 2017.

McMillan, H., Tetzlaff, D., Clark, M., and Soulsby, C.: Do time-variable tracers aid the evaluation of hydrological model structure? A multimodel approach, Water Resources Research, 48, https://doi.org/10.1029/2011WR011688, 2012.

Medici, C., Wade, A. J., and Francés, F.: Does increased hydrochemical model complexity decrease robustness?, Journal of Hydrology, 440–441, 1–13, https://doi.org/10.1016/j.jhydrol.2012.02.047, 2012.

Minville, M., Cartier, D., Guay, C., Leclaire, L.-A., Audet, C., Le Digabel, S., and Merleau, J.: Improving process representation in conceptual hydrological model calibration using climate simulations, Water Resour. Res., 50, 5044–5073, https://doi.org/10.1002/2013WR013857, 2014.

Moazenzadeh, R. and Izady, A.: A hybrid calibration method for improving hydrological systems using ground-based and remotely-sensed observations, Journal of Hydrology, 615, 128688, https://doi.org/10.1016/j.jhydrol.2022.128688, 2022.

Molenat, J., Gascuel, C., Davy, P., and Durand, P.: How to model shallow water-table depth variations: the case of the Kervidy-Naizin catchment -France, Hydrological Processes, 19, 901–920, https://doi.org/10.1002/hyp.5546, 2005.

Hydrology and Earth System Sciences
Discussions

Molenat, J., Gascuel-Odoux, C., Ruiz, L., and Gruau, G.: Role of water table dynamics on stream nitrate export and concentration in agricultural headwater catchment (France), Journal of Hydrology, 348, 363–378, https://doi.org/10.1016/j.jhydrol.2007.10.005, 2008.

Monteil, C., Zaoui, F., Le Moine, N., and Hendrickx, F.: Multi-objective calibration by combination of stochastic and gradient-like parameter generation rules – the caRamel algorithm, Hydrol. Earth Syst. Sci., 24, 3189–3209, https://doi.org/10.5194/hess-24-3189-2020, 2020.

Moussa, R., Chahinian, N., and Bocquillon, C.: Distributed hydrological modelling of a Mediterranean mountainous catchment – Model construction and multi-site validation, Journal of Hydrology, 337, 35–51, https://doi.org/10.1016/j.jhydrol.2007.01.028, 2007.

Nash, J. E. and Sutcliffe, J. V.: River flow forecasting through conceptual models part I — A discussion of principles, Journal of Hydrology, 10, 282–290, https://doi.org/10.1016/0022-1694(70)90255-6, 1970.

Nijzink, R. C., Almeida, S., Pechlivanidis, I. G., Capell, R., Gustafssons, D., Arheimer, B., Parajka, J., Freer, J., Han, D., Wagener, T., van Nooijen, R. R. P., Savenije, H. H. G., and Hrachowitz, M.: Constraining Conceptual Hydrological Models With Multiple Information Sources, Water Resources Research, 54, 8332–8362, https://doi.org/10.1029/2017WR021895, 2018.

Nossent, J., Elsen, P., and Bauwens, W.: Sobol' sensitivity analysis of a complex environmental model, Environmental Modelling & Software, 26, 1515–1525, https://doi.org/10.1016/j.envsoft.2011.08.010, 2011.

Oehler, F., Durand, P., Bordenave, P., Saadi, Z., and Salmon-Monviola, J.: Modelling denitrification at the catchment scale, Science of The Total Environment, 407, 1726–1737, https://doi.org/10.1016/j.scitotenv.2008.10.069, 2009.

Pelletier, A. and Andréassian, V.: On constraining a lumped hydrological model with both piezometry and streamflow: results of a large sample evaluation, Hydrol. Earth Syst. Sci., 26, 2733–2758, https://doi.org/10.5194/hess-26-2733-2022, 2022.

Penman, H. L.: Estimating evaporation, Eos, Transactions American Geophysical Union, 37, 43–50, https://doi.org/10.1029/TR037i001p00043, 1956.

Pesántez, J., Birkel, C., Mosquera, G. M., Célleri, R., Contreras, P., Cárdenas, I., and Crespo, P.: Bridging the gap from hydrological to biogeochemical processes using tracer-aided hydrological models in a tropical montane ecosystem, Journal of Hydrology, 619, 129328, https://doi.org/10.1016/j.jhydrol.2023.129328, 2023.

Pettersson, A., Arheimer, B., and Johansson, B.: Nitrogen Concentrations Simulated with HBV-N: New Response Function and Calibration Strategy, Hydrology Research, 32, 227–248, https://doi.org/10.2166/nh.2001.0014, 2001.

Piovano, T. I., Tetzlaff, D., Carey, S. K., Shatilla, N. J., Smith, A., and Soulsby, C.: Spatially distributed tracer-aided runoff modelling and dynamics of storage and water ages in a permafrost-influenced catchment, Hydrol. Earth Syst. Sci., 23, 2507–2523, https://doi.org/10.5194/hess-23-2507-2019, 2019.

Rajat and Athira, P.: Calibration of hydrological models considering process interdependence: A case study of SWAT model, Environmental Modelling & Software, 144, 105131, https://doi.org/10.1016/j.envsoft.2021.105131, 2021.

Rajib, M. A., Merwade, V., and Yu, Z.: Multi-objective calibration of a hydrologic model using spatially distributed remotely sensed/in-situ soil moisture, Journal of Hydrology, 536, 192–207, https://doi.org/10.1016/j.jhydrol.2016.02.037, 2016.

Rakovec, O., Kumar, R., Mai, J., Cuntz, M., Thober, S., Zink, M., Attinger, S., Schäfer, D., Schrön, M., and Samaniego, L.: Multiscale and Multivariate Evaluation of Water Fluxes and States over European River Basins, Journal of Hydrometeorology, 17, 287–307, https://doi.org/10.1175/JHM-D-15-0054.1, 2016.

Reed, P. and Devireddy, V.: Groundwater monitoring design: a case study combining epsilon dominance archiving and automatic parameterization for the nsga-ii, in: Applications of Multi-Objective Evolutionary Algorithms, vol. Volume 1, WORLD SCIENTIFIC, 79–100, https://doi.org/10.1142/9789812567796_0004, 2004.

Reusser, D. E., Buytaert, W., and Zehe, E.: Temporal dynamics of model parameter sensitivity for computationally expensive models with the Fourier amplitude sensitivity test: TEMPORAL DYNAMICS OF MODEL PARAMETER SENSITIVITY, Water Resour. Res., 47, https://doi.org/10.1029/2010WR009947, 2011.

Riboust, P., Thirel, G., Moine, N. L., and Ribstein, P.: Revisiting a Simple Degree-Day Model for Integrating Satellite Data: Implementation of Swe-Sca Hystereses, Journal of Hydrology and Hydromechanics, 67, 70–81, https://doi.org/10.2478/johh-2018-0004, 2019.

Rinaldo, A., Benettin, P., Harman, C. J., Hrachowitz, M., McGuire, K. J., van der Velde, Y., Bertuzzo, E., and Botter, G.: Storage selection functions: A coherent framework for quantifying how catchments store and release water and solutes: ON STORAGE SELECTION FUNCTIONS, Water Resour. Res., 51, 4840–4847, https://doi.org/10.1002/2015WR017273, 2015.

Saltelli, A.: Making best use of model evaluations to compute sensitivity indices, Computer Physics Communications, 145, 280–297, https://doi.org/10.1016/S0010-4655(02)00280-1, 2002.

Saltelli, A. and Annoni, P.: How to avoid a perfunctory sensitivity analysis, Environmental Modelling & Software, 25, 1508–1517, https://doi.org/10.1016/j.envsoft.2010.04.012, 2010.

Saltelli, A., Tarantola, S., and Chan, K. P.-S.: A Quantitative Model-Independent Method for Global Sensitivity Analysis of Model Output, Technometrics, 41, 39–56, https://doi.org/10.1080/00401706.1999.10485594, 1999.

Saltelli, A., Chan, and Scott: Sensitivity Analysis, 2009.

Seibert, J.: Multi-criteria calibration of a conceptual runoff model using a genetic algorithm, Hydrol. Earth Syst. Sci., 4, 215–224, https://doi.org/10.5194/hess-4-215-2000, 2000.

Seibert, J., Rodhe, A., and Bishop, K.: Simulating interactions between saturated and unsaturated storage in a conceptual runoff model, Hydrol. Process., 17, 379–390, https://doi.org/10.1002/hyp.1130, 2003.

Seibert, J., Grabs, T., Köhler, S., Laudon, H., Winterdahl, M., and Bishop, K.: Linking soil- and stream-water chemistry based on a Riparian Flow-Concentration Integration Model, Hydrology and Earth System Sciences, 13, 2287–2297, https://doi.org/10.5194/hess-13-2287-2009, 2009.

Shafii, M., Craig, J. R., Macrae, M. L., English, M. C., Schiff, S. L., Van Cappellen, P., and Basu, N. B.: Can Improved Flow Partitioning in Hydrologic Models Increase Biogeochemical Predictability?, Water Resources Research, 55, 2939–2960, https://doi.org/10.1029/2018WR024487, 2019.

Shah, S., Duan, Z., Song, X., Li, R., Mao, H., Liu, J., Ma, T., and Wang, M.: Evaluating the added value of multi-variable calibration of SWAT with remotely sensed evapotranspiration data for improving hydrological modeling, Journal of Hydrology, 603, 127046, https://doi.org/10.1016/j.jhydrol.2021.127046, 2021.

Shin, M.-J. and Kim, C.-S.: Assessment of the suitability of rainfall–runoff models by coupling performance statistics and sensitivity analysis, Hydrology Research, 48, https://doi.org/10.2166/nh.2016.129, 2017.

Silvestro, F., Gabellani, S., Rudari, R., Delogu, F., Laiolo, P., and Boni, G.: Uncertainty reduction and parameter estimation of a distributed hydrological model with ground and remote-sensing data, Hydrology and Earth System Sciences, 19, 1727–1751, https://doi.org/10.5194/hess-19-1727-2015, 2015.

Song, X., Zhang, J., Zhan, C., Xuan, Y., Ye, M., and Xu, C.: Global sensitivity analysis in hydrological modeling: Review of concepts, methods, theoretical framework, and applications, Journal of Hydrology, 523, 739–757, https://doi.org/10.1016/j.jhydrol.2015.02.013, 2015.

Stadnyk, T. A. and Holmes, T. L.: Large scale hydrologic and tracer aided modelling: A review, Journal of Hydrology, 618, 129177, https://doi.org/10.1016/j.jhydrol.2023.129177, 2023.

Strohmenger, L., Fovet, O., Akkal-Corfini, N., Dupas, R., Durand, P., Faucheux, M., Gruau, G., Hamon, Y., Jaffrezic, A., Minaudo, C., Petitjean, P., and Gascuel-Odoux, C.: Multitemporal Relationships Between the Hydroclimate and Exports of Carbon, Nitrogen, and Phosphorus in a Small Agricultural Watershed, Water Resour. Res., 56, https://doi.org/10.1029/2019WR026323, 2020.

https://doi.org/10.5194/hess-2023-292
Preprint. Discussion started: 5 January 2024

Strohmenger, L., Fovet, O., Hrachowitz, M., Salmon-Monviola, J., and Gascuel-Odoux, C.: Is a simple model based on two mixing reservoirs able to reproduce the intra-annual dynamics of DOC and NO3 stream concentrations in an agricultural headwater catchment?, Science of The Total Environment, 794, 148715, https://doi.org/10.1016/j.scitotenv.2021.148715, 2021.

Sun, X., Croke, B., Jakeman, A., and Roberts, S.: Benchmarking Active Subspace methods of global sensitivity analysis against variance-based Sobol' and Morris methods with established test functions, Environmental Modelling & Software, 149, 105310, https://doi.org/10.1016/j.envsoft.2022.105310, 2022.

Sutanudjaja, E. H., van Beek, L. P. H., de Jong, S. M., van Geer, F. C., and Bierkens, M. F. P.: Calibrating a large-extent high-resolution coupled groundwater-land surface model using soil moisture and discharge data: CALIBRATING GROUNDWATER-LAND SURFACE MODEL, Water Resour. Res., 50, 687–705, https://doi.org/10.1002/2013WR013807, 2014.

Taylor, P. G. and Townsend, A. R.: Stoichiometric control of organic carbon–nitrate relationships from soils to the sea, Nature, 464, 1178–1181, https://doi.org/10.1038/nature08985, 2010.

Tong, R., Parajka, J., Salentinig, A., Pfeil, I., Komma, J., Széles, B., Kubáň, M., Valent, P., Vreugdenhil, M., Wagner, W., and Blöschl, G.: The value of ASCAT soil moisture and MODIS snow cover data for calibrating a conceptual hydrologic model, Hydrology and Earth System Sciences, 25, 1389–1410, https://doi.org/10.5194/hess-25-1389-2021, 2021.

Tunaley, C., Tetzlaff, D., Lessels, J., and Soulsby, C.: Linking high-frequency DOC dynamics to the age of connected water sources, Water Resources Research, 52, 5232–5247, https://doi.org/10.1002/2015WR018419, 2016.

Viaud, V., Santillàn-Carvantes, P., Akkal-Corfini, N., Le Guillou, C., Prévost-Bouré, N. C., Ranjard, L., and Menasseri-Aubry, S.: Landscape-scale analysis of cropping system effects on soil quality in a context of crop-livestock farming, Agriculture, Ecosystems & Environment, 265, 166–177, https://doi.org/10.1016/j.agee.2018.06.018, 2018.

Wang, A. and Solomatine, D. P.: Practical Experience of Sensitivity Analysis: Comparing Six Methods, on Three Hydrological Models, with Three Performance Criteria, Water, 11, 1062, https://doi.org/10.3390/w11051062, 2019.

Wang, S., Zhang, Z., Sun, G., Strauss, P., Guo, J., Tang, Y., and Yao, A.: Multi-site calibration, validation, and sensitivity analysis of the MIKE SHE Model for a large watershed in northern China, Hydrology and Earth System Sciences, 16, 4621–4632, https://doi.org/10.5194/hess-16-4621-2012, 2012.

Werth, S. and Güntner, A.: Calibration analysis for water storage variability of the global hydrological model WGHM, Hydrology and Earth System Sciences, 14, 59–78, https://doi.org/10.5194/hess-14-59-2010, 2010.

Woodward, S. J. R., Stenger, R., and Bidwell, V. J.: Dynamic analysis of stream flow and water chemistry to infer subsurface water and nitrate fluxes in a lowland dairying catchment, Journal of Hydrology, 505, 299–311, https://doi.org/10.1016/j.jhydrol.2013.07.044, 2013a.

Woodward, S. J. R., Stenger, R., and Bidwell, V. J.: Dynamic analysis of stream flow and water chemistry to infer subsurface water and nitrate fluxes in a lowland dairying catchment, Journal of Hydrology, 505, 299–311, https://doi.org/10.1016/j.jhydrol.2013.07.044, 2013b.

Woodward, S. J. R., Wöhling, T., Rode, M., and Stenger, R.: Predicting nitrate discharge dynamics in mesoscale catchments using the lumped StreamGEM model and Bayesian parameter inference, Journal of Hydrology, 552, 684–703, https://doi.org/10.1016/j.jhydrol.2017.07.021, 2017.

WRB, I.-W.: World reference base for soil resources, World soil resources reports, 103, 1–128, 2006.

Yadav, M., Wagener, T., and Gupta, H.: Regionalization of constraints on expected watershed response behavior for improved predictions in ungauged basins, Advances in Water Resources, 30, 1756–1774, https://doi.org/10.1016/j.advwatres.2007.01.005, 2007.

Yang, H., Choi, H., and Lim, H.: Applicability Assessment of Estimation Methods for Baseflow Recession Constants in Small Forest Catchments, Water, 10, 1074, https://doi.org/10.3390/w10081074, 2018.

https://doi.org/10.5194/hess-2023-292
Preprint. Discussion started: 5 January 2024

Yassin, F., Razavi, S., Wheater, H., Sapriza-Azuri, G., Davison, B., and Pietroniro, A.: Enhanced identification of a hydrologic model using streamflow and satellite water storage data: A multicriteria sensitivity analysis and optimization approach, Hydrological Processes, 31, 3320–3333, https://doi.org/10.1002/hyp.11267, 2017.

Yen, H., Bailey, R. T., Arabi, M., Ahmadi, M., White, M. J., and Arnold, J. G.: The Role of Interior Watershed Processes in Improving Parameter Estimation and Performance of Watershed Models, Journal of Environmental Quality, 43, 1601–1613, https://doi.org/10.2134/jeq2013.03.0110, 2014.